RESEARCH ARTICLE

Ecology and Evolution
Open Access WILEY

Transcriptomic thermal plasticity underlying gonadal development in a turtle with ZZ/ZW sex chromosomes despite canalized genotypic sex determination

Thea B. Gessler[1,2] | Zhiqiang Wu[1,3] | Nicole Valenzuela[1]

[1]Department of Ecology, Evolution, and Organismal Biology, Iowa State University, Ames, Iowa, USA

[2]Genetics and Genomics Program, Iowa State University, Ames, Iowa, USA

[3]Guangdong Laboratory for Lingnan Modern Agriculture, Agricultural Genomics Institute at Shenzhen, Chinese Academy of Agricultural Sciences, Shenzhen, China

Correspondence
Nicole Valenzuela and Thea B. Gessler, Department of Ecology, Evolution, and Organismal Biology, Iowa State University, Ames, Iowa, USA.
Email: nvalenzu@iastate.edu and tgessler@iastate.edu

Abstract

Understanding genome-wide responses to environmental conditions during embryo-genesis is essential for discerning the evolution of developmental plasticity and canalization, two processes generating phenotypic variation targeted by natural selection. Here, we present the first comparative trajectory analysis of matched transcriptomic developmental time series from two reptiles incubated under identical conditions, a turtle with a ZZ/ZW system of genotypic sex determination (GSD), *Apalone spinifera*, and a turtle with temperature-dependent sex determination (TSD), *Chrysemys picta*. Results from our genome-wide, hypervariate gene expression analysis of sexed embryos across five developmental stages revealed that substantial transcriptional plasticity in the developing gonads can persist for >145 Myr, long after the canalization of sex determination via the evolution of sex chromosomes, while some gene-specific thermal sensitivity drifts or evolves anew. Such standing thermosensitivity represents an underappreciated evolutionary potential harbored by GSD species that may be co-opted during future adaptive shifts in developmental programing, such as a GSD to TSD reversal, if favored by ecological conditions. Additionally, we identified novel candidate regulators of vertebrate sexual development in GSD reptiles, including sex-determining candidate genes in a ZZ/ZW turtle.

KEYWORDS
eco-evo-devo adaptation, embryonic transcriptomes, plasticity versus canalization, sex determination by temperature and sex chromosomes, turtle reptile vertebrates

TAXONOMY CLASSIFICATION
Genomics

1 | INTRODUCTION

Understanding the evolution of developmental plasticity and canalization is a fundamental question, as these alternative trajectories generate incredible phenotypic variation targeted by natural selection and driving biodiversity (Beldade et al., 2011; Gomez-Mestre & Buchholz, 2006; Matesanz et al., 2010). In developmental plasticity, environmental cues shape the phenotypic fate of an individual, rather than genes alone, whereas canalized development is robust to environmental perturbation (West-Eberhard, 2003). Why some organisms evolve developmental programs susceptible to the whims of the environment remains a fascinating question. Evolutionary theory

predicts that when the ecological environment provides reliable cues for phenotypic matching, developmental plasticity increases organismal fitness and is thus adaptive (West-Eberhard, 2003). Yet, how these external cues are translated into the molecular signals underlying developmental plasticity is not fully known, nor how regulatory networks become insensitive to environmental inputs in canalized systems. This gap hinders our understanding of the evolution of plasticity (or lack thereof) at a molecular level and of the consequences of environmental change.

Sex determination, the commitment to male or female developmental fate, occurs by numerous mechanisms that vary in their level of plasticity (Bachtrog et al., 2014; Bull, 1983; Valenzuela, 2018) and impacts population dynamics by producing initial sex ratios (Abreu-Grobois et al., 2020; Bull, 1983). Sex-determining mechanisms (SDMs) span a spectrum from strictly canalized systems of genotypic control (genotypic sex determination–GSD), such as by sex chromosomes, to plastic mechanisms under virtually complete environmental control (ESD), such as temperature-dependent sex determination (TSD) commonly found in reptiles (Bachtrog et al., 2011; Kratochvíl et al., 2021; Tree of Sex Consortium, 2014).

Turtles are a vertebrate lineage where both GSD and ESD co-occur (Bachtrog et al., 2014; Stöck et al., 2021) although not within any species studied so far (Mu et al., 2015; Valenzuela et al., 2014). Temperature-dependent sex determination predominates in turtles and is the likely ancestral state from which GSD evolved multiple times independently as XX/XY or ZZ/ZW systems of sex chromosomes (Bista & Valenzuela, 2020; Janzen & Krenz, 2004; Organ & Janes, 2008; Sabath et al., 2016), which may have been lost in some turtle lineages that reverted back to TSD (Literman et al., 2018; Valenzuela & Adams, 2011). Whether TSD is adaptive in turtles remains the focus of theoretical and empirical research (Schwanz & Georges, 2021; Valenzuela, 2021) as does the evolution of turtle sex chromosomes and their dosage compensation (Bista et al., 2021; Bista & Valenzuela, 2020; Rovatsos & Kratochvíl, 2021). In TSD turtles, the incubation temperatures experienced by the embryo around the middle third of development determine whether the bipotential gonads develop into testes or ovaries by influencing molecular and cellular processes (Merchant-Larios et al., 2021). This thermosensitive period represents the window of time when the environmental temperatures affect sex ratios the most (Bull & Vogt, 1981), although temperatures before this canonical period can also have an influence (albeit lesser) (Gómez-Saldarriaga et al., 2016; Valenzuela, 2001). Most turtles develop as males at colder temperatures and as females at warmer temperatures (TSDIa or MF pattern) (Ewert et al., 2004). Thus, turtle sex determination affords an ideal opportunity to study phenotypic plasticity and canalization in an eco-evo-devo framework.

Here, we leverage and expand turtle genomic resources to investigate the evolution of the molecular architecture underlying contrasting SDMs, and test for evolutionary shifts in thermosensitivity at the transcriptional level. For this, we compare genome-wide gene expression during embryogenesis in a GSD and a TSD turtle. Our data permit detangling, for the first time, the effects

of sex and temperature on transcription in a turtle with sex chromosomes to illuminate how and why sexual development is plastic in some taxa and canalized in others. Our approach includes RNA-sequencing from matched samples of *Chrysemys picta* (TSD) and *Apalone spinifera* (GSD), two species from the suborder Cryptodira (referred to by their genus names hereafter). *Apalone* belongs to the family Trionychidae, which lost developmental plasticity for sex determination, replacing it with a ZZ/ZW sex chromosome system ~161–145 mya (timetree.org) (Badenhorst et al., 2013; Literman et al., 2018; Rovatsos et al., 2017). *Chrysemys* serves as a proxy for the ancestral plastic sex determination (Bista et al., 2021). Despite the loss of thermal influence on sex ratio, *A. mutica* and *A. spinifera* exhibit relic and derived thermosensitivity in the expression of some genes (Radhakrishnan et al., 2017, 2018; Valenzuela, 2008a, 2008b; Valenzuela et al., 2013), which could be acted upon by natural selection during future adaptation. Unfortunately, these earlier studies could not disentangle the effects of temperature and sex on gene expression because methods to diagnose the sex of embryos (Literman et al., 2014, 2017) were developed after those studies were conducted. This gap obscures our understanding of the molecular architecture and plasticity underlying both the development of a basic sexual dimorphism (the commitment and differentiation of the gonads) and its evolution with and without sex chromosomes.

To address these questions, we pioneer the application of trajectory analysis (Adams & Collyer, 2009) to a developmental time series of RNA-seq datasets, to gain insight on global patterns of gene expression that can be elusive otherwise. Specifically, we test how the hyperdimensional path of global gene expression through developmental time differs between colder and warmer incubation temperatures in a TSD turtle (*Chrysemys*), and how this trajectory is influenced by sex, temperature, and their interaction in a GSD turtle (*Apalone*). We then provide a biological interpretation of the plasticity (or lack thereof) of these transcriptional embryonic trajectories.

2 | MATERIALS AND METHODS

2.1 | Sample collection

Freshly laid eggs of *Chrysemys* and *Apalone* were collected from turtle farms in Iowa and Oklahoma, respectively, transported to the laboratory soon thereafter, and incubated in the laboratory concurrently and under identical conditions, following standard protocols (Valenzuela, 2009). Briefly, eggs were randomly assigned to incubation boxes and kept at 4% humidity by replacing lost water weekly or before removing eggs. Two constant temperatures were used, 26°C and 31°C, which are within the optimal range for both species and are typically used in studies of their development (Bull & Vogt, 1979, 1981; Gutzke et al., 1987). In *Chrysemys*, 26°C is a male-producing temperature (MPT) and 31°C is a female-producing temperature (FPT) (Bull & Vogt, 1981), whereas *Apalone* produces both sexes at these values (Bull & Vogt, 1979) given their ZZ/

ZW sex chromosome system (Badenhorst et al., 2013). Embryos of both species were dissected at five identical embryonic stages (Yntema, 1968) to obtain matching samples for comparison. The following tissues were collected for gene expression analysis: trunks at stage 9, adrenal kidney gonad complexes (AKG) at stages 12 and 15, and gonads at stages 19 and 22. In stage 9 embryos, the gonadal primordium cannot be separated in the trunks. In stage 12 embryos, the genital ridge may be present in the AKGs as observed in *Trachemys scripta* turtles (Spotila et al., 1998). And at stage 15, the gonads could not be separated from the AK, lack distinctive internal structure in *Apalone* (Greenbaum & Carr, 2001) and consistently, are bipotential in *Chrysemys* (Bull & Vogt, 1981). In *Chrysemys*, stages 9 and 12 precede the sex-determining thermosensitive period (TSP), stage 15 lies right before the TSP, while stages 19 and 22 fall within the mid- and late-TSP, respectively (Bull & Vogt, 1981). The sex of *Apalone* embryos was assessed by PCR amplification of sex-linked markers (Literman et al., 2017), permitting unambiguous diagnosis of individual sex in a simpler manner than by qPCR of rDNA repeats (Literman et al., 2014). *Chrysemys* embryos were presumed to be developing-males or -females if incubated at the MPT or FPT, respectively (Bull & Vogt, 1981). Thus, our sampling permits comparing global gene expression of the same tissues in TSD versus GSD species at equivalent stages of development, corresponding to before and during the thermosensitive period of the TSD taxon. We note that because tissues sampled differ by stage, results through time should be interpreted with caution.

Total RNA was extracted from collected tissues using RNeasy Kits (Qiagen), quantified using a NanoDrop1 ND-1000 Spectrophotometer, and evaluated for quality by the presence of ribosomal RNA bands in agarose gels stained with ethidium bromide. For *Apalone*, two pools of RNA (biological replicates) per sex were generated per stage and temperature by dividing male or female embryos into two groups of similar or equal size (5–10 embryos per pool). For *Chrysemys*, two pools per temperature per stage were obtained in the same manner using 11–15 embryos per pool. This pooling design captures and accounts for biological variation among individuals which strengthens the differential gene expression analysis. Equal amounts of total RNA per embryo were added to obtain 1 µg RNA per pool, and shipped to Duke Genome Sequencing Core (DUGSIM) for RNA-seq library preparation and sequencing. The KAPA Stranded mRNA-seq kit (KK8421) was used on the Sciclone Liquid Handling Workstation to prepare the RNA libraries. RNA libraries were sequenced using Illumina's HiSeq 4000 with 150 bp paired-end reads. At least 42 M reads were generated per library (average 54 M reads) from which a minimum of 40 M clean reads were obtained (average 52 M reads, or 94%–97% retention rate per library). These correspond to the RNAseq data used in two prior partial analyses of *Dmrt1* splicing and expression in *Chrysemys* (Mizoguchi & Valenzuela, 2020) and of sex chromosome dosage compensation in *Apalone* (Bista et al., 2021). The analyses presented here are distinct from these previous studies and use the full RNAseq datasets for the first time, including a direct between-species comparison of genome-wide transcriptional patterns.

2.2 | Transcriptome assembly

Briefly, FASTQ paired-end reads were quality trimmed using Trimmomatic (v0.36) (Bolger et al., 2014), concatenated, normalized to a maximum coverage of 30 (Trinity v2.6.6) (Grabherr et al., 2011), and mapped using GSNAP (v20170317) (Wu & Nacu, 2010; Wu & Watanabe, 2005) to the reference *Chrysemys* genome assembly (GCF_000241765.3_Chrysemys_picta_bellii-3.0.3) (Badenhorst et al., 2015) and to our in-house *Apalone* genome assembly (BioProject: PRJNA837702). For the alignment of normalized reads, the novel splicing feature was turned on (-N 1), and a mismatch of seven was allowed (−m 7). This level of mismatch is more conservative than the maximum recommended (−m 10) and resulted in the highest mapping rate. This value was chosen to accommodate the highly heterozygous reads expected from libraries that encompass multiple individuals as described above, which contain a broad representation of the genetic variation present in natural populations. The SAM file of each alignment was converted to a BAM file using Samtools (v1.4) (Li, 2011; Li et al., 2009), and the BAM file was assembled de novo using a genome guided approach as implemented in Trinity (v2.6.6) (Grabherr et al., 2011) with a max intron size of 10,000 and a kmer size of 32. Additional details and parameters used in these steps can be found in the supplementary scripts file.

2.3 | Generating final reference transcriptome assembly and annotations

Initial transcriptome fragmentation and redundancy were reduced using TransPS (v1.1.0) (Huang et al., 2016; Liu et al., 2014) for transcript-protein scaffolding on blastx (Camacho et al., 2009) top hits. Prior to running TransPS with default parameters, duplicate copies were removed from the reference proteome using CD-HIT (v4.6.8) (Fu et al., 2012; Li & Godzik, 2006). Additionally, all blastx results were first reoriented into the sense direction using seqtk (v1.2) (github.com/lh3/seqtk). Top hits from blastx were filtered by best bit score and e-value and retained for downstream analysis. Transcripts that failed the initial blastx to *Chrysemys* proteins were blasted against chicken (GCF_000002315.6_GRCg6a_protein.faa), the closest vertebrate with the highest quality and well-annotated genome available. Finally, we used blastn against the RNACentral database (version 11) (The RNAcentral Consortium, 2019) to annotate non-coding RNA (ncRNA) present among orphan transcripts. The final reference assembly was also blasted against the Uniprot vertebrate database (SwissProt v12-18-2019) (The UniProt Consortium, 2018) to correct occasional name discrepancies in the *Chrysemys* annotations, primarily for the enrichment analysis and weighted gene co-expression network analysis (WGCNA) described below. To assess assembly quality before and after scaffolding, BUSCO (v2.0) (Simão et al., 2015) scores were calculated utilizing the Tetrapoda database from Orthodb (v9) (Zdobnov et al., 2016), and read representation in the assembly was determined using GSNAP and Samtools. The SAM file was converted to a BAM file using Samtools, and flagstat was

run to determine mapping rates (Table S1). Sequences with >10% Ns were removed from the reference transcriptome prior to differential expression analysis (i.e., 4.2% of reference transcripts for *Chrysemys* and 5.7% for *Apalone*). Additional details are provided in the supplementary scripts file.

2.4 | Differential expression analysis

Kallisto (v0.46.0) (Bray et al., 2016) was used to obtain counts for the final reference assembly from the trimmed reads which were pseudo-aligned to the final transcriptome assembly (indexed with a kmer of 31) (see supplementary scripts file for details). Pseudo-alignment rates (Table S1) were comparable between the raw Trinity assembly and the TransPS assembly. Differential expression analyses were conducted on these counts for each developmental stage separately in the R (v3.5.0) (R Core Development Team, 2018) package DESeq2 (v1.20.0) (Love et al., 2014) using a custom script. Differential expression was calculated between temperatures (26°C vs 31°C) for *Chrysemys*. For *Apalone*, differential expression was modeled at each stage using a full factorial analysis (Y ~ temp × sex) to evaluate differential expression between 26°C and 31°C (temperature effect), between males and females (sex effect), and the temperature-by-sex interaction. Because the interaction was nonsignificant for embryonic stages 9, 12, and 15 for most genes, a reduced model (Y ~ temp + sex) was applied to evaluate only temperature and sex effects at those stages. All differentially expressed genes (DEGs) were identified using a corrected *p*-value <.05.

The transcriptomes of *Chrysemys* were validated by comparing TPM values to previously published qPCR expression data (Mizoguchi & Valenzuela, 2020; Valenzuela et al., 2013) and to previously published transcriptomes (Mizoguchi & Valenzuela, 2020; Radhakrishnan et al., 2017), to assess the similarity of expression patterns for six genes of interest at identical incubation conditions [*Aromatase* (*Cyp19a*), *Sf1* (*Nr5a1*), *Wt1*, *Dax1* (*Nr0b1*), *Sox9*, and *Dmrt1*] across the five embryonic stages, and to other genes from previous studies that used different RNAseq data (Radhakrishnan et al., 2017, 2018). For *Apalone*, validation was conducted to assess the similarity of expression patterns of these genes across development, by comparing TPM values of the same six genes of interest between temperatures only (modeled as Y ~ temp) to the previously published transcriptomic studies that only examined thermal effects on gene expression (Radhakrishnan et al., 2017, 2018).

We analyzed patterns of overlap of DEGs using the R package VennDiagram (v1.6.20) (Chen, 2018). For *Chrysemys*, we identified DEGs with consistent patterns across embryonic stages, whereas for *Apalone*, we identified DEGs by temperature and by sex. Then, we compared a set of reciprocal best blast hits between *Chrysemys* to *Apalone* to identify DEGs with consistent patterns between species at each stage, and genes with sexually dimorphic expression in *Apalone* that may or may not be thermosensitive in *Chrysemys*, to uncover instances of evolutionary retention, gain, or loss of thermosensitivity. Based on these results, we built working hypotheses

of potential gene candidates important for sex determination in *Apalone*, and especially those that might contribute to the transition from TSD to GSD in the softshell turtle lineage.

2.5 | Trajectory analysis

Gene expression profiles are highly multivariate data, composed of the expression values for all genes per pool of individuals per treatment through time (Adams & Collyer, 2009; Collyer & Adams, 2013), and can be thought of as a temporal trajectory of gene expression (phenotypic response values) over the five embryonic stages. This approach permits the analysis of hyperdimensional genome-wide expression trajectories, whereas alternative existing approaches address gene-by-gene patterns in RNAseq time series (Oh & Li, 2021). First, an ANOVA was conducted to investigate how the genome-wide transcriptomic response (means of the principal components of gene expression for all replicate RNA-seq libraries) differed between temperatures in *Chrysemys*, and how they differed in *Apalone* by temperature, sex, and their interaction. A significant interaction term (*p*-value <.05) suggested the presence of biological interactions for which trajectory analysis is useful to interpret. For this, the resulting multivariate trajectories of gene expression were analyzed for differences in their attributes of magnitude (distance), direction (angle), and shape in the multidimensional gene expression space (Adams & Collyer, 2009; Collyer & Adams, 2013; Figure 1). Although we applied this approach to qPCR data for six genes of interest previously (Valenzuela, 2010), to our knowledge, this is the first application of trajectory analysis at the global transcriptome-level for developmental time series data. Following procedures outlined by Adams and Collyer (2009), embryonic trajectories of gene expression for both *Chrysemys* and *Apalone* were assessed using the R (v3.5.0) package RRPP (v0.4.2) (Collyer & Adams, 2018). When interpreting these results, we kept in mind that different tissues were analyzed at different stages of development, such that some changes in the trajectories may be attributable to tissue differences. Additionally, as trajectories are hyperdimensional, visual projections in lower dimensions were interpreted with caution, and always corroborated by other data.

Briefly, for the trajectory analysis here, trimmed mean of M values (TMM) normalization (Robinson & Oshlack, 2010) was applied using Trinity to render expression values comparable across libraries. Gene expression values were then $\log_2$ transformed to correct for heteroskedasticity, after adding 0.0001 to all counts to avoid dividing by zero in downstream calculations, and the positive effect of this correction was visualized by comparing the results from a principal components analysis (PCA) performed before and after the transformation (results not shown). Data were fit to a general linear model (*Chrysemys*: gene_expression ~ temperature*stage; *Apalone*: gene_expression~ temperature-sex*stage) using lm.rrpp(), and significance assessed by ANOVA. Trajectory analysis was run in RRPP using trajectory.analysis(), and trajectories were evaluated for differences in magnitude, direction, and shape, using a
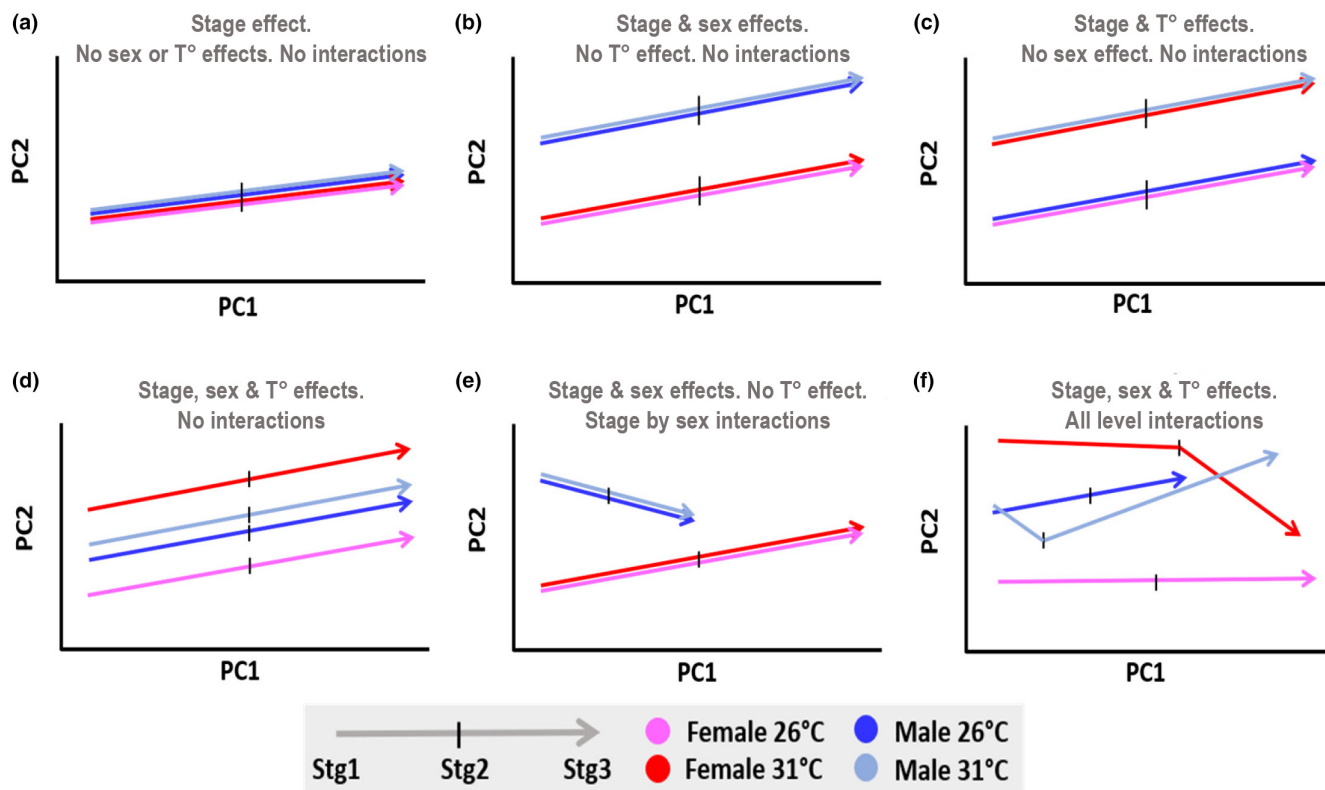
FIGURE 1 Hypothetical potential results from the trajectory analysis. Panels illustrate a few simplified examples of trajectories over three developmental stages of male and female embryos of a GSD species incubated at two temperatures. All trajectories in (a–d) are of equal magnitude, angle, and shape. Male and female trajectories in (e) differ in both magnitude and angle. Trajectories in panel f differ in magnitude, angle, and shape. Other examples can be found in (Collyer & Adams, 2007).

Bonferroni-corrected alpha (applied with p.adjust()) when multiple hypotheses were tested on the same dataset (which was the case for *Apalone*).

2.6 | Enrichment analysis

Mapping to the UniProt database (described above) was performed prior to enrichment analysis. For *Chrysemys*, 25,527 of 29,607 gene models in the reference transcriptome had a hit in SwissProt, and 18,084 had a GO ID associated with that annotation. For *Apalone*, 23,246 of 25,696 gene models in the reference transcriptome had a hit in SwissProt, and 16,849 had a GO ID associated with that annotation. Higher gene model numbers in *Chrysemys* and *Apalone* are due to the annotation of isoforms present in the *Chrysemys* and/or chicken protein sequences used for assembly redundancy reduction and annotation.

Enrichment analyses were run using Ontologizer (v2.1) (Bauer et al., 2008). Model-based gene set analysis (MGSA) was used as the calculation method (Bauer et al., 2010), ignoring genes without associations between genes and GO Terms (option -i). Gene Ontology files required to run the enrichment analysis were downloaded from geneontology.org on 01/08/2020 (Ashburner et al., 2000; The Gene Ontology Consortium, 2019). For *Chrysemys*, the enrichment was

calculated for DEGs that were upregulated at MPT [26°C-biased] and at FPT [31°C-biased]. For *Apalone*, enrichment was calculated for DEGs that were male-biased at 26°C, male-biased at 31°C, female-biased at 26°C, female-biased at 31°C, and alternatively, for genes that were 26°C-biased in males, 26°C-biased in females, 31°C-biased in males, 31°C-biased in females, using the same $\log_2$(FoldChange) relationship as for *Chrysemys*.

2.7 | Weighted gene correlation network analysis—WGCNA

To test for the presence of modules in the gene regulatory network of sexual development, we employed the WGCNA R package (v1.69) (Langfelder & Horvath, 2008; Zhang & Horvath, 2005) to construct (i) a turtle consensus network, (ii) a *Chrysemys*-specific network, and (iii) an *Apalone*-specific network from reciprocal best blast hits between the two transcriptomes. To construct the modules, we followed guidance provided by the online tutorials (https://horvath.genetics.ucla.edu/html/CoexpressionNetwork/Rpackages/WGCNA/Tutorials/). Counts were rounded to integers, filtered to a minimum cross-library read count of at least 20, and transformed using varianceStabilizingTransformation() from the DESeq2 package. Data were then cleaned and clustered, and a soft-power of 8

was selected as it best met the assumption of a scale-free topology. Then, consensus and species modules were built.

Weighted gene correlation network analysis uses (1) correlation to measure co-expression and thus, interaction among genes; (2) hierarchical clustering to identify co-expression modules (highly correlated groups of genes); and (3) eigengene network analysis to define module relationships (Langfelder & Horvath, 2008). Briefly, network nodes are gene expression profiles, edges between genes are the pairwise correlations between their gene expression, and connectivity is how highly co-expressed a gene is relative to other genes in a module (Langfelder & Horvath, 2008). A module's eigengene is its principal component, or representative (weighted average) gene expression profile. When interpreting gene co-expression data, we are mindful that these species-specific networks are based on highly heterogeneous data that vary by sex, temperature, and embryonic stage/tissue, which could influence the construction of networks.

Overlap between consensus and species-specific modules (and the genes involved) were calculated, as well as the network adjacency (i.e., connection strength between nodes) and preservation (i.e., conservation or similarity) among species-specific modules. Given the high conservation of the vertebrate sex determination network (Merchant-Larios et al., 2021; Morrish & Sinclair, 2002), we predicted that high module overlap would exist, but also that some differences in the molecular circuitry of TSD and GSD mechanism would be present between _Chrysemys_ and _Apalone_.

3 | RESULTS

3.1 | Transcriptome assembly and validation

A large fraction of reads mapped to the reference genomes: 94.27% for _Chrysemys_ and 86.18% for _Apalone_. Raw Trinity assemblies contained >1 M transcripts with high redundancy. These were reduced to 29,607 gene models for _Chrysemys_ and 25,696 for _Apalone_ using TransPS with minimal loss of data pre- and postscaffolding, less duplication, and greater completeness based on BUSCO scores (Table S1). Furthermore, pseudocounts from Kallisto were only slightly lower after running TransPS indicating that a similar amount of data was utilized in both cases (Table S1). The final transcriptome for each species had BUSCO scores of 93.90% and 91.50% for complete transcripts, respectively (Table S1). Validation of the resulting reference transcriptomes using six genes of interest [_Wt1_, _Sf1 (Nr5a1)_, _Dax1 (Nr0b1)_, _Sox9_, _Aromatase (Cyp19a1)_, _Dmrt1_] profiled earlier (Mizoguchi & Valenzuela, 2020; Radhakrishnan et al., 2017; Valenzuela et al., 2013) revealed similar expression profiles from all datasets (Figure 5), with only two exceptions detected for _Chrysemys_ between transcriptomic studies [(Radhakrishnan et al., 2017) and this study]. Similarly, using the simpler model (Y ~ temp) in _Apalone_ that disregarded sex information revealed similar results for the same six genes to previous analyses using unsexed embryos (Table S19) for stages 9–15, but differences for stages 19 and 22 were observed.

Namely, the simple model detected no differential expression by temperature in stage 19 and 22 gonads, likely because differences due to sex and temperature were confounded and canceled each other out in the previous study (Radhakrishnan et al., 2017). Thus, sexing _Apalone_ embryos and using more embryos per library here, provided greater sensitivity to detect differential expression of gene regulators of vertebrate gonadogenesis than before (Radhakrishnan et al., 2017).

3.1.1 | Wilms tumor 1

Because the _Wt1_ genomic sequence is split between two scaffolds in the _Chrysemys_ reference genome, we validated _Wt1_ expression patterns using the _Trachemys_ genome as a reference (GCF_013100865.1_CAS_Tse_1.0_genomic.fna). In _Trachemys_, _Wt1_ contains three annotated isoforms X1, X2, and X3, which correspond to a sequence with KTS (+KTS), a sequence without KTS (-KTS), and a short sequence containing KTS (+KTS-short). Reads that had mapped to _Chrysemys'_ two _Wt1_ fragments and to the scaffold containing _Wt1_ in _Apalone_ were extracted and analyzed using the same pipeline described for our main analysis. Results using _Trachemys_ as reference corroborated our main results overall. Namely, both _Chrysemys_ and _Apalone_ expressed primarily two _Wt1_ isoforms, +KTS and +KTS-short, but _Chrysemys_ favored +KTS, whereas _Apalone_ favored +KTS-short. This pattern agrees with our original result showing expression of two _Wt1_ isoforms, one more highly expressed in _Chrysemys_ and the other in _Apalone_.

3.2 | ANOVA and trajectory analysis uncover transcriptional dimorphism and thermal plasticity in _Apalone_

Given the complex and multivariate nature of transcriptomic data, trajectory analysis was used to understand the significant interaction terms in the genome-wide transcriptional responses identified via ANOVA (Table 1—All Genes). For _Chrysemys_, we found that developmental stage, temperature, and their interaction all had a significant effect on the expression of DEGs, at a Benjamini–Hochberg corrected $\alpha < 0.05$, whereas only stage was significant when genome-wide transcription was included, likely because subtler signals in DEGs were masked by the noise from genes with monomorphic expression (Table 1—DE Genes). In _Apalone_, data were divided into sex-by-temperature subsets (26°C-female, 31°C-female, 26°C-male, 31°C-male) and all ANOVA terms were significant, both genome-wide and DEGs only (Table 1). Below, we compare trajectories between species for the DEGs.

For _Chrysemys_, gene expression trajectories differed in magnitude (the amount of change exhibited by DEGs), direction (the sets of DEGs), and shape (changes in magnitude and/or direction through two or more embryonic stages) (Table 2; Figure 2a,c,e). For _Apalone_ (Table 2), results from the trajectory analysis across

TABLE 1 Results of ANOVA of gene expression in *Chrysemys picta* and *Apalone spinifera* genome-wide or for DEGs only.

Gene set	Factor	Z score	*p*-value
Chrysemys picta			
All Genes: Stages 9–22	Temperature	1.3167	.1030
	Stage	5.5806	**.0005**
	Interaction	0.3574	.3950
DE Genes: Stages 9–22	Temperature	2.1528	**.0265**
	Stage	5.4237	**.0005**
	Interaction	3.6743	**.0005**
Apalone spinifera			
All Genes: Stages 9–22	TempSex	1.8544	**.0455**
	Stage	9.8548	**.0005**
	Interaction	2.2748	**.0075**
DE Genes: Stages 9–22	TempSex	3.2104	**.001**
	Stage	8.7623	**.0005**
	Interaction	6.4318	**.0005**

Note: For *Chrysemys*, the model tested the effect of temperature, stage, and their interaction, whereas for *Apalone* the model tested the effect of sex-by-temperature, stage, and their interaction. Significant *p*-values are denoted in bold italics.

all embryonic stages were consistent with the sex-by-temperature interaction identified by ANOVA. Namely, the trajectories across stages (Figure 2b,d,f) exhibited similar magnitude, but the direction of change differed between males and females at 31°C (sex effect), and between temperatures for males (temperature effect), revealing differences in the set of genes that were differentially expressed. Furthermore, temperature affected the shape of the female trajectories under 26°C and 31°C, indicating consecutive changes in magnitude and or direction across two or more embryonic stages. Analyzing *Apalone*'s data with the model used for *Chrysemys* (excluding sex as a factor) revealed that the lack of magnitude differences in *Apalone* was explained by our detangling of the effects of sex and temperature on development in this GSD turtle.

The first principal component (PC1) of the trajectory analysis for both species captures mostly developmental time (Figure 2a,b). Plotting PC3 versus PC1 and PC3 versus PC2 for *Chrysemys* reveals divergence by temperature (Figure 2c,d), which is captured by directional differences between trajectories. For stages 9 and 12 (trunks and AKGs, respectively), trajectories are primarily parallel, but by the onset of the TSP (stage 15) sexually dimorphic transcription becomes evident in the AKGs, is accentuated through stage 19 gonads, and lessens by stage 22 in the gonads, the end of *Chrysemys*' TSP (Bull & Vogt, 1981). Genes influencing the trajectories the most are listed in Tables S2 and S3, which for *Chrysemys* included many transcriptional regulators (*Eloa1, Tet1, Nr5a2, Smarca2, Tcf7l2, Rbfox2, and Zic4*), whereas in *Apalone*, fewer genes had higher impact and these included genes associated with development (*Lhx2* and *Dgcr2*).

Our *Apalone* data permitted disentangling temperature effects from sex effects in a GSD turtle for the first time. Indeed, the plots

PC3 versus PC1 and PC3 versus PC2 depict sex and temperature effects (Figure 2d,f). Alike *Chrysemys*, stages 9–12 trajectories are mostly parallel in *Apalone*, although a potential temperature effect on magnitude is observed by stage 12. Male and female trajectories re-converge at stage 15 (although a temperature effect remains evident). Angular variation increases later due to thermal responses within each sex, and both sex and temperature contribute to the divergence of the trajectories at stages 19–22, with sexually dimorphic transcription accentuated under warmer conditions, whereas male and female gene expression is less dimorphic at 26°C. Developing ovaries were more thermally plastic at stages 19–22, whereas testicular transcription was more canalized at stage 19 and more thermosensitive at stage 22. Generally, gene expression differences are most extreme at stage 22 for *Apalone* and at stage 19 for *Chrysemys*.

3.3 | Enrichment analysis

The enrichment analysis revealed no consistent shared GO terms between species (see Table S4). All cases of enrichment that spanned multiple developmental stages in *Chrysemys* were observed at FPT, and included oxidation–reduction process, among others. Two of eight stage-spanning cases in *Apalone* were enriched in females and not by temperature, and the other six occurred in males. Interestingly, the terms enriched by temperature in *Apalone* never spanned multiple stages.
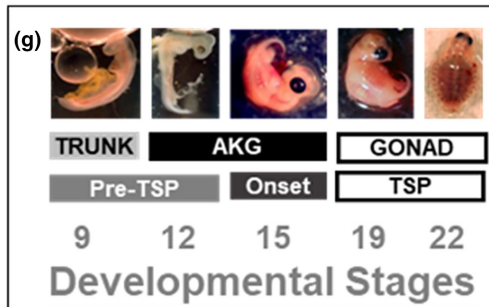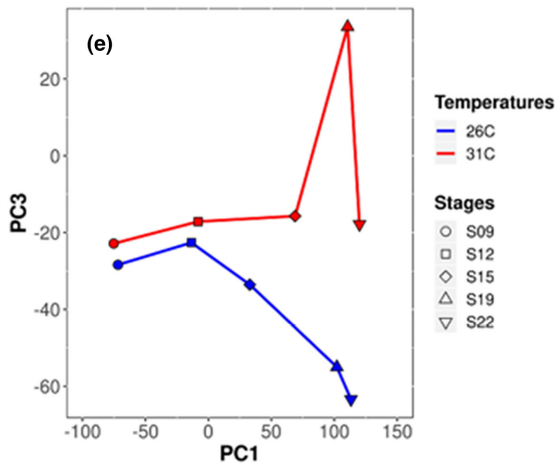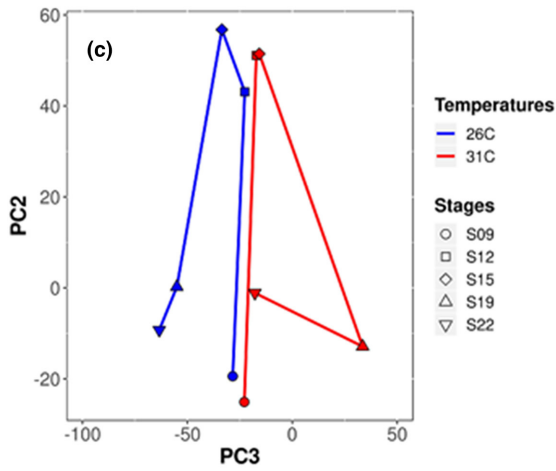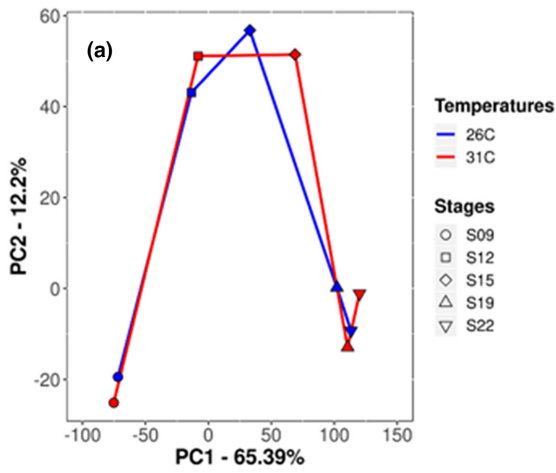
3.4 | Species comparisons reveal candidate sex-determining genes in *Apalone* with canalized sex-specific expression in GSD turtles

Around half of *Chrysemys* DEGs between temperatures occurred at a single developmental stage, mostly in the AKGs at the onset of the TSP (stage 15) and in the gonads at mid-TSP (stage 19). A larger number of DEGs occurred across multiple stages during the TSP than before (Figure 3a), perhaps because stages 9–15 contained mixed tissues. Full lists of DEGs are presented in the Tables S5 and S6.
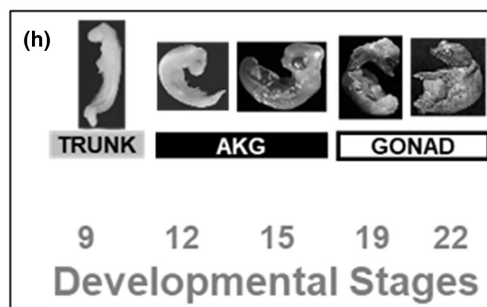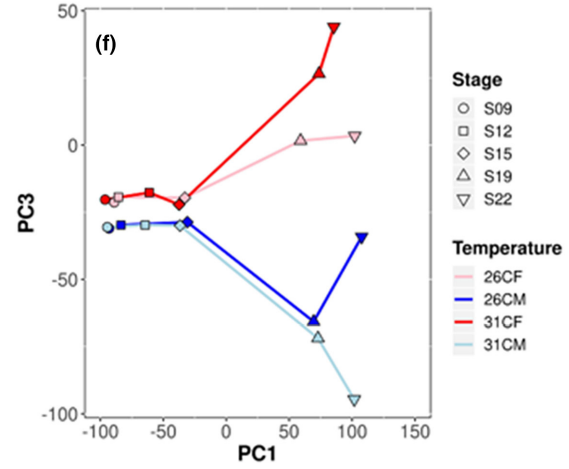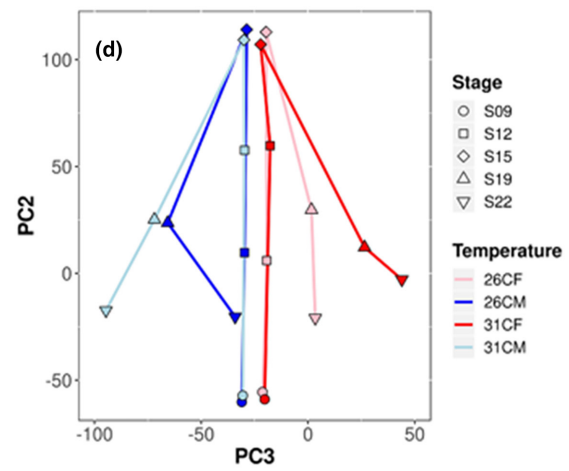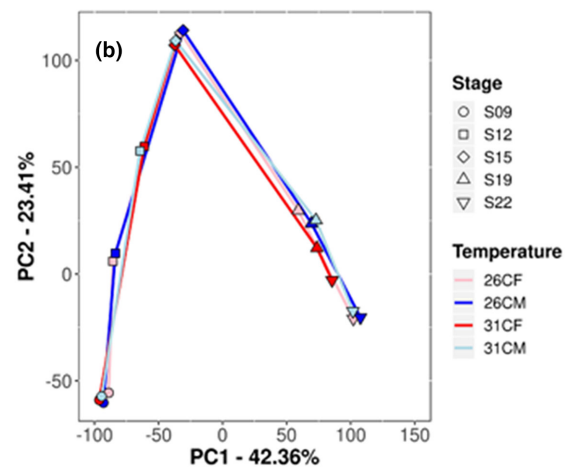
In *Apalone*, most DEGs occurred between temperatures and fewer between sexes at stages 9–15, with negligible sex-by-temperature interaction (<20 genes per stage), highlighting considerable thermal plasticity (either retained or derived) in the trunks and AKGs of this GSD species (Figure 3b–d). By contrast, genes in gonads at stages 19–22 (which correspond to the mid and late-TSP of *Chrysemys*) showed a significant sex-by-temperature interaction in *Apalone* (360 and 1314 genes, respectively). For full lists of genes, see Table S7 and S8.

Cross-species analysis of DEGs by stage (Figure 4) uncovered numerous genes that are thermosensitive in *Chrysemys* (TSD) but not in *Apalone* (GSD), except at stage 12 (Figure 4b), when DEGs in *Chrysemys* are less abundant relative to other stages. Interestingly, there are also many thermosensitive DEGs unique to *Apalone* (Figure 4), especially at stages 19–22 (Figure 4d,e), yet many were

Chrysemys picta (left column: a, c, e, g) and *Apalone spinifera* (right column: b, d, f, h). PCA plots showing PC1, PC2, PC3 components and developmental stages (S09, S12, S15, S19, S22) across temperatures (26C, 31C) with panels (g) and (h) showing Developmental Stages 9, 12, 15, 19, 22.

FIGURE 2 Principal component plots of multivariate gene expression trajectories of *Chrysemys picta* and *Apalone spinifera*. Principal components PC1, PC2, and PC3 are presented from 26°C (blue) and 31°C (red) treatments for *Chrysemys* (left panels a,c,e) and for 26°C-females (pink), 26°C-males (blue), 31°C-females (red), and 31°C-males (light-blue) for *Apalone* (right panels b,d,f). Panels illustrate PC1 vs PC2 (a,b), PC2 vs PC3 (c,d), and PC1 vs PC3 (e,f). Embryonic stages sampled are illustrated in panels g and h: *Chrysemys* photos from our lab; softshell photos reproduced from (Tokita & Kuratani, 2001) (stages 9–12 *Pelodiscus sinensis*) and from (Greenbaum & Carr, 2002) (stages 15–22 *Apalone spinifera*) with permission.

TABLE 2 Results of trajectory analysis for *Chrysemys picta* and *Apalone spinifera*.

Stages compared	Attribute of change	Z score	p-value or Bonferroni corrected p-value	Effect type
Chrysemys picta				
Stages 9–22	Magnitude	3.446172	*.0025*	
	Direction	4.721982	*.0005*	
	Shape	2.634093	*.0095*	
Apalone spinifera				
Stages 9–22	Direction: 26CF:31CM	4.479990	*.006*	Sex and temperature
	Direction: 26CM:31CF	4.403077	*.003*	Sex and temperature
	Direction: 26CM:31CM	3.148147	.054	Temperature
	Direction: 31CF:31CM	5.206589	*.003*	Sex
	Shape: 26CF:31CF	3.525388	*.009*	Temperature
	Shape: 26CF:31CM	2.539313	*.048*	Sex and temperature
	Shape: 26CM:31CF	2.652483	.051	Sex and temperature

Note: Results include effect sizes (z scores) and significance of trajectory attributes (magnitude, direction, and shape). For *Apalone* significance was corrected for multiple comparisons, and type of effect detected is presented based on pairwise comparisons. Significant *p*-values are denoted in bold italics, whereas *p*-values in regular font are marginally significant (<.055).

differentially expressed by sex also. For full lists of genes see Tables S9–S13.

Importantly, we identified seven novel candidate sex-determining genes in *Apalone* which lost thermosensitivity relative to *Chrysemys* and exhibit early sex-specific expression at stage 9 (*Rrp8, Clh1*) and stage 15 (*S26a1, Sc5a1, Msi1h, Sat2, Ppil2*). Substantially more genes showed this pattern (loss of thermosensitivity accompanied by sexually dimorphic expression) at later stages in *Apalone* (Stage 19: 597 genes, Stage 22: 347 genes), revealing significant canalization of gonadogenesis at stages equivalent to *Chrysemys* TSP when plastic responses are observed. For full lists of genes, see Tables S9–S13.

Our approach offered greater sensitivity to detect differential expression for known gene regulators of vertebrate gonadogenesis (Figure 6; Table 3). Among these, we note that the testis differentiation gene *Dhh* entirely reverses its expression pattern between the two species. It shows upregulation at 31°C throughout *Chrysemys* TSP, whereas in *Apalone*, *Dhh* is upregulated at 26°C during those same stages but is male-biased at stages 19–22 (Figure 6). Furthermore, because response to stress may mediate the evolution of ESD in amniotes (Straková et al., 2020), we searched qualitatively for genes annotated as related to stress response (response to cold, response to heat), present in the transcriptomes of *Chrysemys* (175 genes) and *Apalone* (167 genes) (Ashburner et al., 2000; The Gene Ontology Consortium, 2019), and showing consistent pattern across at least three stages. In *Chrysemys*, 17 such stress-DEGs were

detected, including several heat-shock proteins and *Cirbp* (a TSD candidate gene upregulated in *Chrysemys* across all stages) upregulated at 31°C, and four genes upregulated at 26°C (Table S14). In *Apalone*, only 1 gene (*Atp2a2*, a gene implicated in calcium transport) was male-upregulated across stages 9–15 (Table S15). For stages 19–22 in *Apalone*, many stress-related candidates for sexual development (Straková et al., 2020) were detected at 26°C, including *Ano1*, *Atp2a2*, *Ppargc1a*, *Sst*, *Tgfb1i1*, and *Fosl2*. Interestingly, all stress DEGs found in *Chrysemys* were both differentially expressed by sex and by temperature at some stage in *Apalone*.

3.5 | WGCNA point to part conserved and part evolutionarily labile regulation underlying turtle sexual development

Broad similarities and differences between *Chrysemys* and *Apalone* were detected using WGCNA that help formulate working hypotheses for further studies by identifying groups of highly co-expressed genes within species (species-specific modules) and across species (consensus modules) as detailed in the Tables S16–S18. Not surprisingly, species level networks contained fewer and larger modules (*Chrysemys*: 8 modules; *Apalone*: 12 modules) than the consensus network across species (24 modules) (Figure 7a,b). Modular co-expression preservation (conservation) between species is illustrated
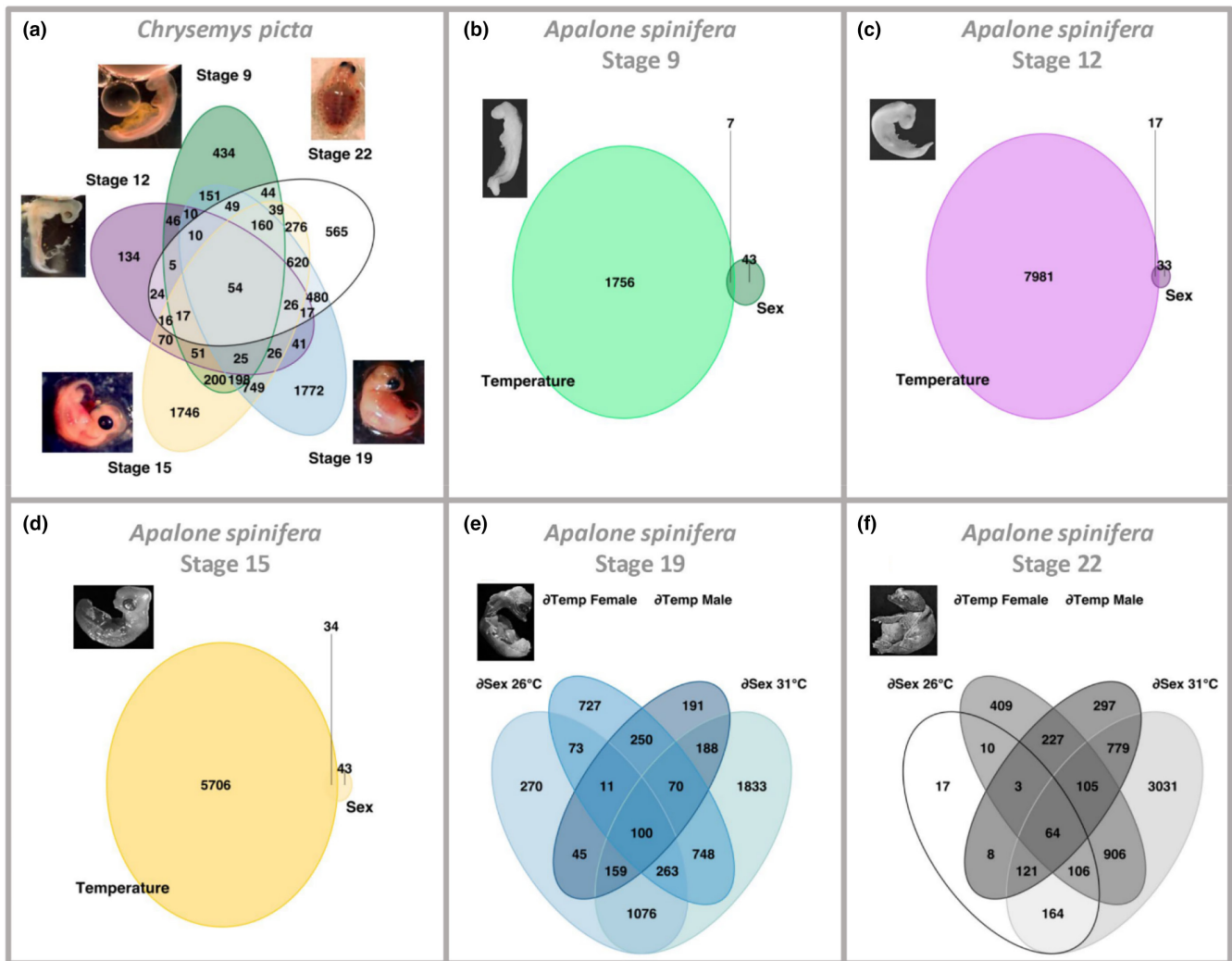
FIGURE 3 Venn diagrams illustrating the overlap of differentially expressed genes (DEGs) between developmental stages of _Chrysemys picta_ and _Apalone spinifera_. DEG overlap across stages for _Chrysemys_ (a). DEG overlap for _Apalone_ between conditions (sex vs. temperature) at stages 9 (b), 12 (c), 15 (d), 19 (e), and 22 (f). ∂ = between. ∂Sex 26°C = DEGs between males and females incubated at 26°C. ∂Sex 31°C = DEGs between males and females incubated at 31°C. ∂Temp Female = DEGs between 26°C and 31°C in females. ∂Temp Male = DEGs between 26°C and 31°C in males.

in Figure 8. Importantly, the correlation pattern of consensus modules is not always preserved between species, revealing changes in co-expression patterns of groups of genes across taxa. Indeed, in several cases, consensus modules assigned to a single _Chrysemys_ module (Figure 7a) were less correlated within _Apalone_ (Figure 7b). Yet, we also found evidence of preservation of CPI-1 and CPI-6 modules within _Apalone_, but weak to moderate for CPI-3, CPI-4, CPI-5, and CPI-7, and none for CPI-2 and CPI-8 (note that modules were independently constructed in _Apalone_, such that module number ID do not indicate the same module between taxa). Thus, only some modular structure is preserved between the two species.

We examined the module membership of several genes that are interesting known candidates for a role in sex determination to determine whether any showed similar co-expression patterns indicative of a cooperative role. We observed that _Wt1_, _Ar_, _Esr1_, and _Kdm6b_ all belong to consensus module Cons-24; _Sox9_ and _Dmrt1_ belong to

Cons-11; and _Amh_ and _Rrp8_ belong to Cons-23, revealing consensus modules with distinct member elements that are conserved across species. By contrast, _Aromatase_, numerous epigenetic regulatory genes such as _Dicer_, _Ago2_, _Dnmt1_, and several histone demethylases belong to Cons-14, the module with the lowest preservation in co-expression patterns between species, indicating that the connections of these elements within the sexual development network are evolutionarily labile. Furthermore, _Sf1_ and _Trpv4_ were not observed in any consensus modules, and their failure to pass the reciprocal best blast hit filter applied, indicates their DNA sequences may have diverged between _Chrysemys_ and _Apalone_. Among the most highly connected gene (top hub genes) for each module (Table 4), whose expression profile is highly representative of the module's expression profile (the module's eigengene) (Langfelder & Horvath, 2008), we note genes linked to stress response and epigenetic regulation (_Hmgb1_, _Ndrg1_, _Smca5_ and _Piwil4_).
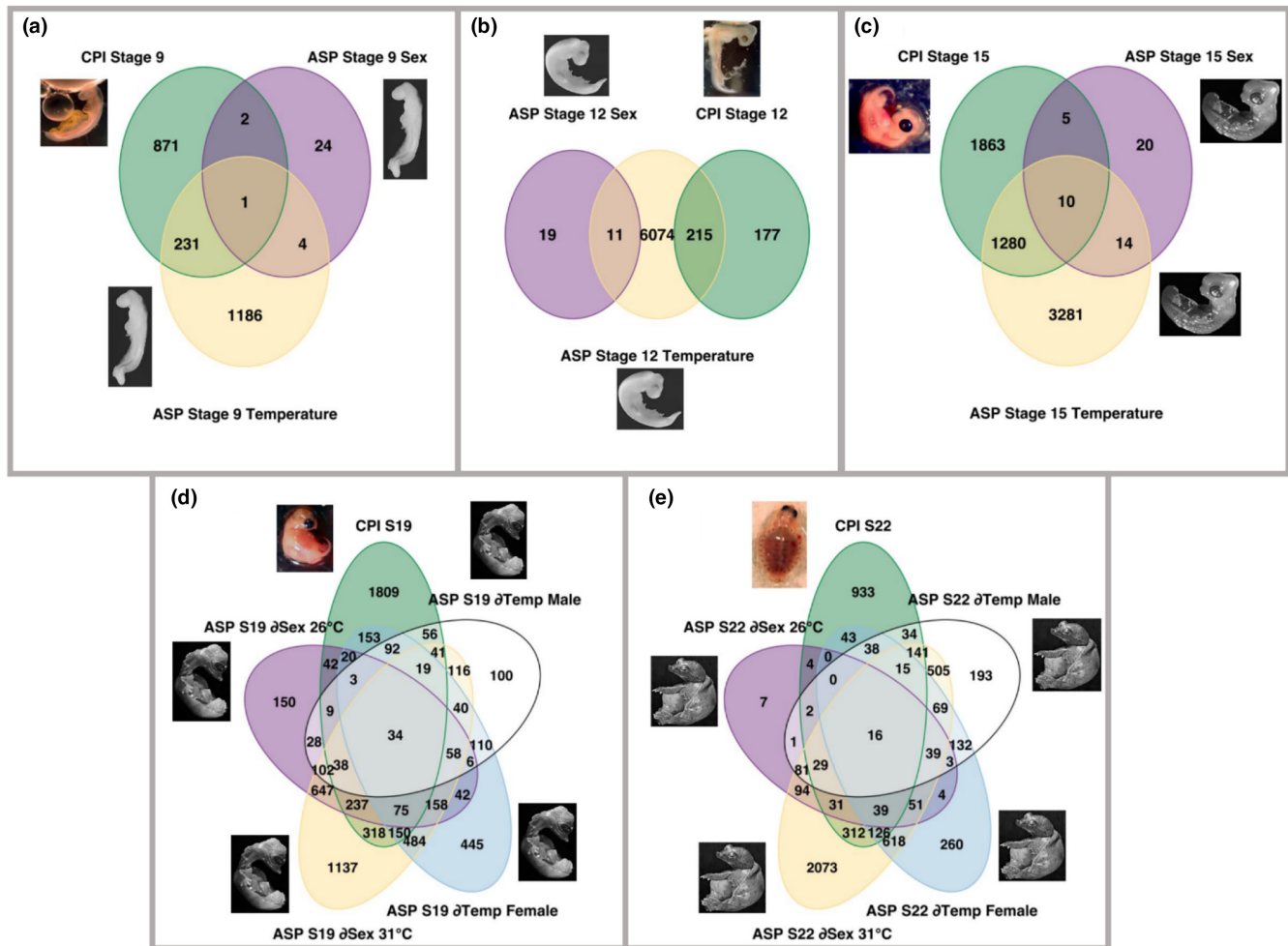
FIGURE 4 Venn diagrams of the overlap of differentially expressed genes (DEGs) between *Apalone* and *Chrysemys* at stage 9 (a), 12 (b), 15 (c), 19 (d), and 22 (e). *Apalone* data are grouped into DEGs by temperature and DEGs by sex for stages 9–15 (a–c), and by temperature and sex in a full factorial analysis (d and e). ∂ = between. ∂Sex 26°C = DEGs between males and females incubated at 26°C. ∂Sex 31°C = DEGs between males and females incubated at 31°C. ∂Temp Female = DEGs between 26°C and 31°C in females. ∂Temp Male = DEGs between 26°C and 31°C in males.

4 | DISCUSSION

Understanding the evolution of vertebrate sex determination is hampered because studies of sex-specific genome-wide transcription during gonadal development in lineages with evolutionarily labile sex determination have been restricted to TSD taxa. Here, we present the first ever transcriptomic analysis of sexed embryos of a GSD turtle with sex chromosomes (*Apalone*), incubated at two temperatures that produce only males or females in a TSD counterpart (*Chrysemys*). Our study informs the molecular circuitry changes that accompanied the loss of plastic sex determination in *Apalone*'s lineage (Trionychidae) during the evolution of ZZ/ZW sex chromosomes (Badenhorst et al., 2013) from the ancestral TSD condition (Bista et al., 2021; Sabath et al., 2016) represented by *Chrysemys*. Our data uncovered sex-specific transcriptional patterns underlying sexual development in *Apalone*, and thermal plasticity in this GSD species at stages corresponding with the TSP in *Chrysemys*, a window of time that is fairly conserved across TSD turtles (thus, likely ancestral), and

which encompasses approximately the middle third of development (Valenzuela, 2001, 2008). Importantly, the greatest differences between species were detected in the individual gonads (stages 19–22) compared with mixed tissues (stages 9–15), underscoring the divergence in gonadogenesis separating these turtle lineages. Our results are conservative because subtle patterns in the early developing gonad could be masked by expression of nongonadal tissues.

Several nonmutually exclusive factors may drive the observed thermal plasticity in *Apalone*. First, some thermal sensitivity may be relic from its TSD ancestor, which would be reflected in DEGs with similar expression between *Apalone* and *Chrysemys*, as occurs for the male development gene *Wt1* (Valenzuela, 2008b; Valenzuela et al., 2013). Second, some thermal sensitivity in *Apalone* may have diverged via developmental systems drift (True & Haag, 2001), and by genetic drift, since the costs of transcription in eukaryotes are typically low (Lynch & Marinov, 2015) [although excessive expression of ribosomal genes in *Apalone* appears costly and undergoes dosage compensation as a consequence (Montiel et al., 2022)]. Drift

TABLE 3 Novel or confirmed differential expression (or lack thereof) in _Chrysemys picta_ and _Apalone spinifera_ of previously studied genes of interest.

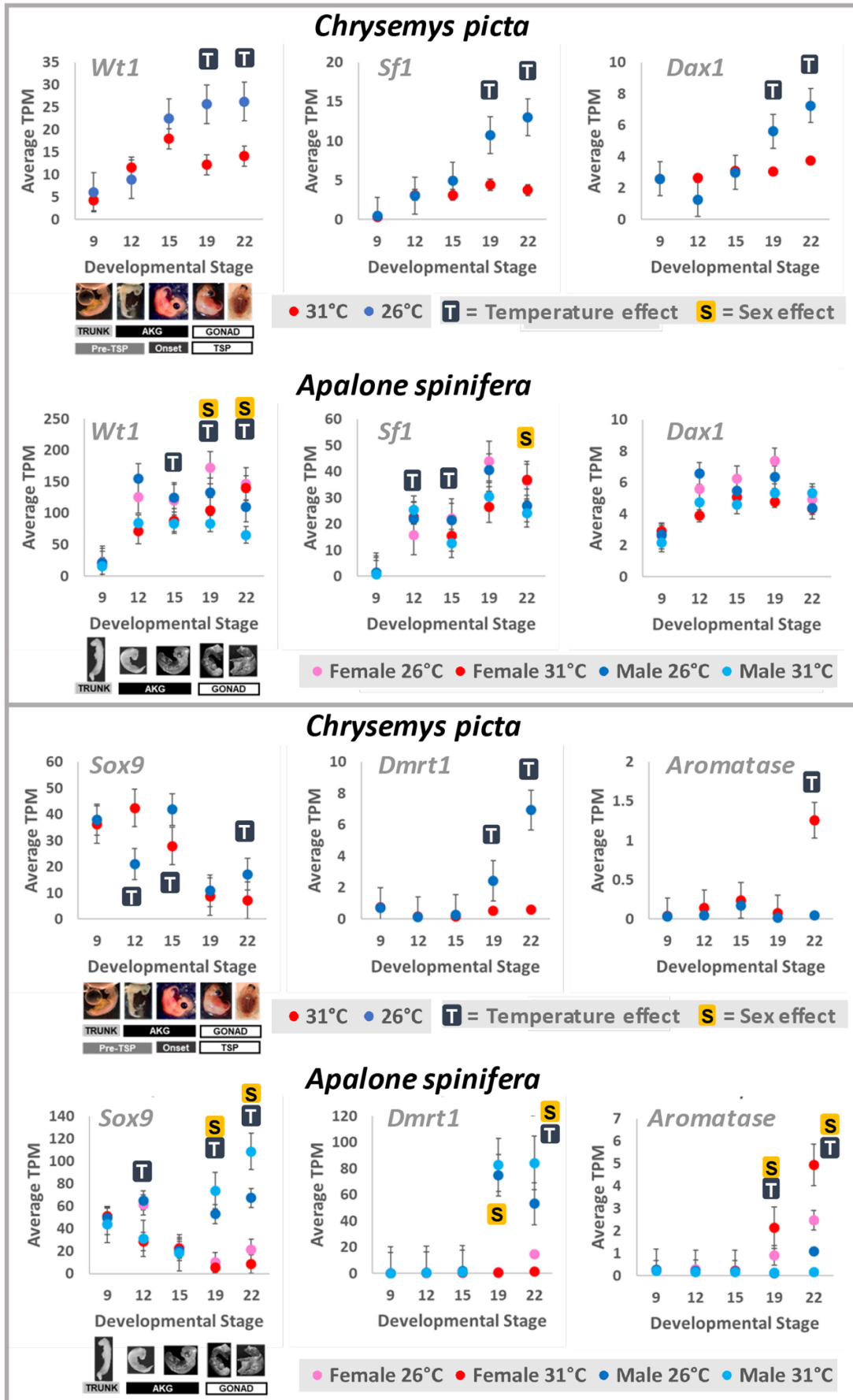| Taxa	Pattern	Genes
CPI	Confirmed upregulation at 26°C (developing male)	_Amh, Dax1, Dmrt1, Dmrt2, Fog2, Gata4, Kdm3a, Lhx9, Sf1, Sox9, Wt1_
	Confirmed upregulation at 31°C (developing female)	_Aromatase, Ctnnb1, Dhh, Foxl2, Gata2, Lhx1, Sox9, Srd5a2_
	Novel differential expression	_Apc, Cbx2, Ctnnb1, Dhh, Fhl2, Gata2, Gata4, Igf1r, Insr, Kdm3a, Lhx1, Lhx9, Ptch1, Six1, Sox9_
	Monomorphic expression across all stages	_Cbln4, Cyp26b1, Dmrt3, Esr2, Rspo1, Wnt4_
ASP	ZW Female upregulation >1 stage	_Aromatase, Ctnnb1, Emx2, Foxl2, Lhx9, Rspo1, Six4, Wt1_
	ZZ Male upregulation >1 stage	_Amh, Dhh, Dmrt1, Dmrt3, Fgfr2, Fog2, Insr, Ptch1, Sox9_
	Thermosensitive	_Amh, Apc, Ar, Aromatase, Cbx2, Ck1, Ctnnb1, Cyp26b1, Dhh, Dmrt1, Dmrt2, Emx2, Esr2, Fgf9, Fgfr2, Fhl2, Fog2, Foxl2, Gata2, Gata4, Igf1r, Insr, Kdm3a, Lhx9, Ptch1, Rspo1, Sf1, Six1, Six4, Sox9, Wnt4, Wt1_

Note: Details in Supplementary excel file.

TABLE 4 Top hub gene found in each _Chrysemys_ and _Apalone_ co-expression module.

Module	Gene symbol	Gene name
Chrysemys		
CPI-1	_Tm35b_	Transmembrane protein 35B
CPI-2	**_Hmgb1_**	High mobility group box 1
CPI-3	_Mat2b_	Methionine adenosyltransferase 2b
CPI-4	_Ddx17_	DEAD-box helicase 17
CPI-5	_Zfhx4_	Zinc finger homeobox protein 4
CPI-6	**_Ndrg1_**	N-myc downstream regulated 1
CPI-7	_Lrc17_	Leucine rich repeat containing 17
CPI-8	_Nomo2_	NODAL modulator 2
Apalone		
ASP-1	**_Smca5_**	SWI/SNF related, matrix associated, Actin dependent regulator of chromatin, subfamily A, member 5
ASP-2	_Lsm7_	LSM7 homolog, U6 small nuclear RNA and mRNA degradation associated
ASP-3	_Zn646_	Zinc finger protein 646
ASP-4	_Lich_	Lipase A, lysosomal acid type
ASP-5	_Lama4_	Laminin subunit alpha 4
ASP-6	_Kat1_	Kynurenine aminotransferase 1
ASP-7	_Metk2_	Methionine adenosyltransferase 2A
ASP-8	_Lmx1a_	LIM homeobox transcription factor 1 alpha
ASP-9	**_Piwil4_**	Piwi like RNA-mediated gene silencing 4
ASP-10	_Fyb2_	FYN binding protein 2
ASP-11	_Jam3_	Junctional adhesion molecule 3
ASP-12	_Lect2_	Leukocyte cell derived chemotaxin 2

Note: Bold italic indicates top hub genes representative of their module's expression profile (module eigengenes) linked to stress response or epigenetic regulation.

FIGURE 5 Transcriptional profiles from this study showing six genes of interest in _Chrysemys picta_ and _Apalone spinifera_. "S" indicates DEGs between sexes and "T" indicates DEGs between temperatures. We note that the DNA sequence of _Wt1_ in the _Chrysemys_ genome v3.0.3 is split across two scaffolds, one containing the KTS region [a tripeptide present or absent in two _Wt1_ splice variants conserved across vertebrates (Hammes et al., 2001)], and the other containing the upstream part of the gene, such that the reference transcriptome contains transcripts of similar expression corresponding to these two sub-regions. We report the partial KTS-containing region here as it is most comparable between species.

Legend — *Chrysemys picta* Upregulation: ● = 26°C, ● = 31°C.
Legend — *Apalone spinifera* Upregulation: ● = 26°C, ● = 31°C, ● = Male, ● = Female.
For *Chrysemys picta* the Sig.Effect is T° (= Sex).

Chrysemys picta 9	12	15	19	22	GENE	*Apalone spinifera* 9 Sex	9 T°	12 Sex	12 T°	15 Sex	15 T°	19 26° Sex	19 31° Sex	19 F T°	19 M T°	22 26° Sex	22 31° Sex	22 F T°	22 M T°
			26	26	AMH							M	M		31		M	26	
		26			APC				26				M						
					AR				31					26					
				31	Aromatase							F	F	31			F		26
					CBLN4														
		26			CBX2				26		31						F		
					CK1														
					CK1						31						F		31
31		26			CTNNB1						31	F	F		26		F		26
					CYP26B1							F		26					
			26	26	DAX1														
	31	31	31	31	DHH						26	M	M	26			M		26
			26	26	DMRT1							M					M		26
		26			DMRT2														
					DMRT3								M				M		
					EMX2				31			F	F		26		F		26
					ESR2					26									
					FGF9				31								F		26
					FGFR2		26		31		31		M						
					FGFR2				31										
					FGFR2														
			26		FHL2				31			F			31				
					FOG2							M	M				M		
				26	FOG2				31										
				31	FOXL2							F	F			F	F		26
	31		31		GATA2				31					26					
					GATA4														
			26	26	GATA4				31	26								26	26
					GSK3B														
			31		IGF1R				26			M	M						
			31		INSR				26				M	26			M		
26		26			KDM3A		31												
			31	31	LHX1														
		26		26	LHX9				31			F	F				F		
		26	26		LHX9				26			26	F	26			F		26
		26			PTCH1				26										
					PTCH1							M					M		
					RSPO1				26			F	F	26					26
			26	26	SF1				31	26							F		
		26			SIX1						31								
					SIX4							F					F		
	31		26	26	SOX9							M	M		31	M	M	26	
				31	SRD5A2														
					WNT4					26		F	F						
				26	WT1-a												F		
					WT1-b				26			F	F						26
			26	26	WT1-partial					26		F	F	26			F		26

FIGURE 6 Genes of interest from the vertebrate sexual development network and their expression pattern by sex and/or temperature. First row indicates the developmental **stage** (9–22), followed by the **group** from the factorial design in *Apalone*, i.e., incubation temperature (26°C or 31°C), and sex (F, Female and M, Male). **Sig (significant) effect T** indicates significant difference between temperature treatments, while **Sex** indicates significant difference between males and females. Red = 31°C; darker blue = 26°C; pink = female; light blue = male. Blank cells denote non-significant effects. WT1-a, WT1-b, and WT1-patial, correspond to protein annotations for isoform sequences X1 and X2 present in the *Chrysemys picta* genome assembly v3.0.3, and the partial Wt1 protein sequences included in Figure 5, respectively (not to the-KTS, +KTS, and +KTS-short discussed in the text).

FIGURE 7 Correspondence of *Chrysemys* (a) and *Apalone* (b) specific modules (genes with highly correlated expression within each species); to consensus modules (genes with highly correlated expression in both species). Numbers within cells indicate the number of genes that overlap between species-specific and consensus modules. Red scale indicates –log(p) where *p* is the Fisher's exact test *p*-value, and greater intensity indicates a more significant overlap between modules.

(a) **Correspondence of CPI-modules and CPI-ASP consensus modules**

(b) **Correspondence of ASP-modules and CPI-ASP consensus modules**
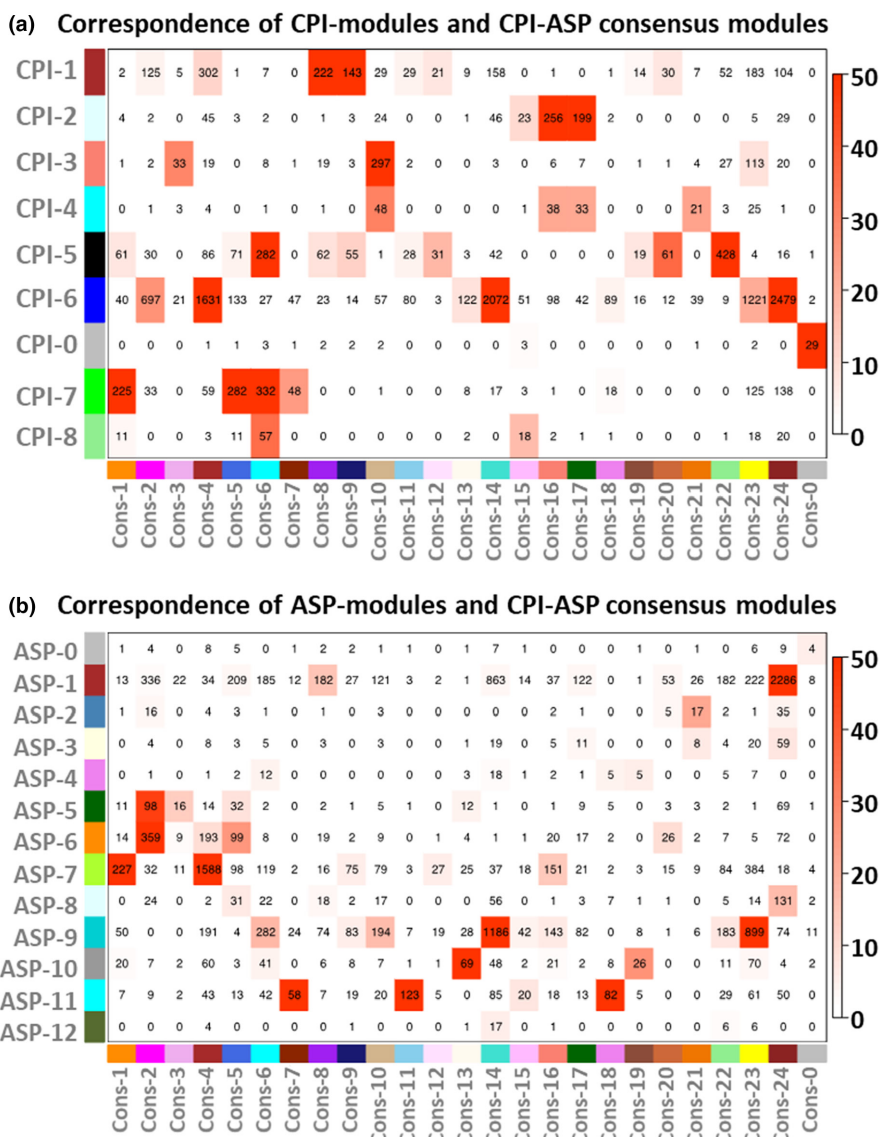
would be reflected in genes with thermosensitive expression but of different pattern between species, such as *Dhh*, a testis differentiation gene upregulated at 31°C across stages in *Chrysemys* and at 26°C in *Apalone* during stages 19–22 in our study. Genes whose thermosensitivity in *Apalone* evolved by drift are probably unimportant for sex determination or sexual differentiation, or compensated for in another way (e.g., during translation), as those costs may be sufficiently high to be visible to selection (Lynch & Marinov, 2015). Third, some thermal sensitivity may be entirely novel in either *Apalone* or *Chrysemys* and have arisen after their lineages split from each other. Lastly, it should

be noted that not all transcriptional thermal plasticity may function in sex determination or sexual differentiation, and some may simply be due to the exotherm biology of these reptiles. These differences should be kept in mind when interpreting the discussion below. For instance, thermal plasticity in *Apalone* even surpasses that in *Chrysemys* in the number of DEGs by temperature at early stages and is particularly prominent at stage 12 (Figure 3), which is especially intriguing as it is decoupled from sexual development in this GSD species. Whichever its source, thermal sensitivity harbored by GSD taxa over evolutionary time may serve as raw material for natural

selection to act upon during future adaptation, including potential reversals to TSD. Such scenarios may have occurred in other turtle lineages, including the TSD sister to softshell turtles, _Carettochelys_

insculpta (Literman et al., 2018; Valenzuela & Adams, 2011), precluding their use as proxy for the TSD pattern ancestral to softshells. Thus, given that all other TSD cryptodiran turtles are equally distant
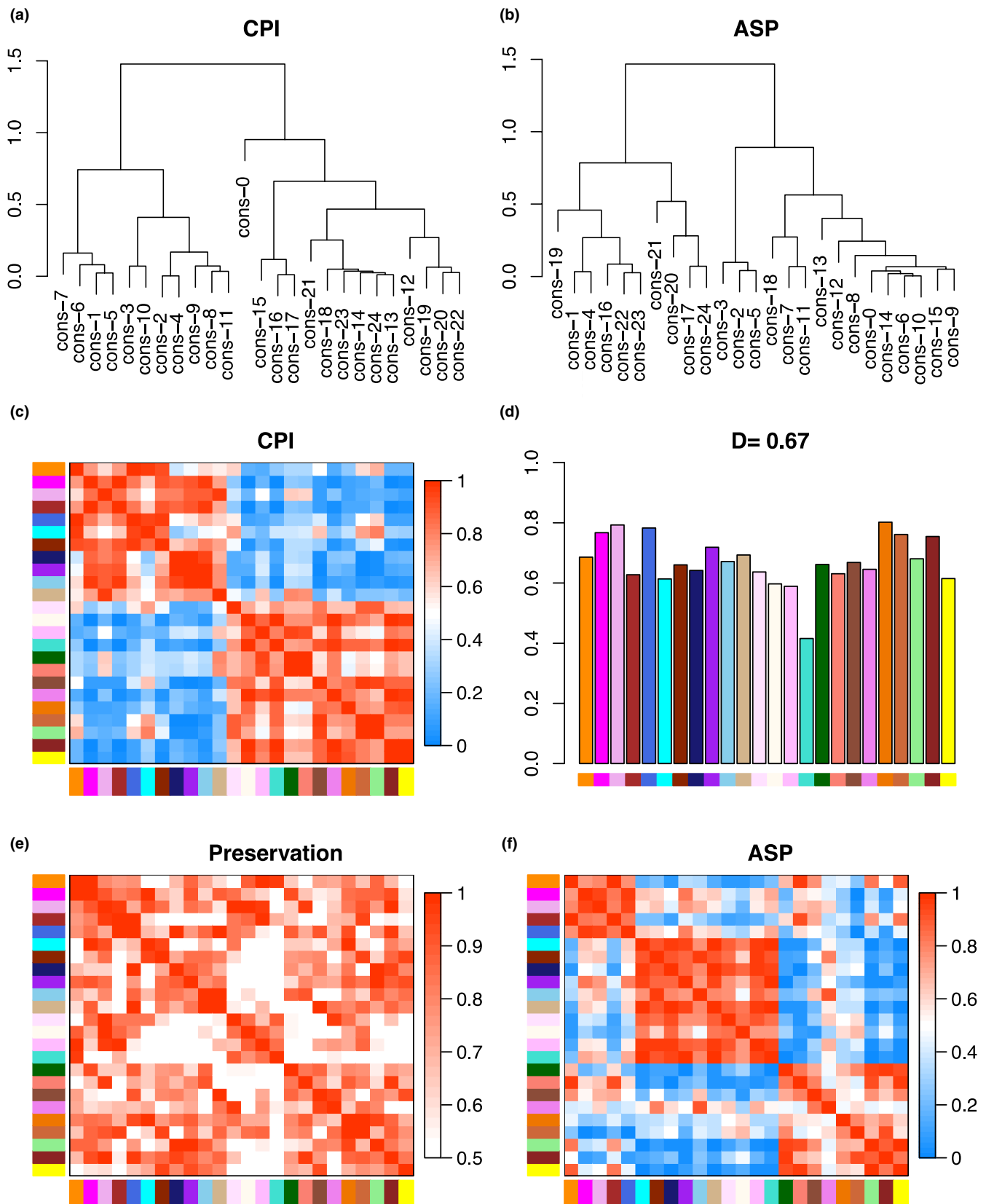
FIGURE 8 WGCNA results comparing *Chrysemys* and *Apalone* to each other. (a) Clustering for *Chrysemys* and (b) *Apalone* of consensus gene co-expression modules. Panels (c) (for *Chrysemys*) and (f) (for *Apalone*) contain heatmaps of eigengene networks (interconnectivity plots) which summarize the relationship among module co-expression patterns within species by clustering their eigengenes (weighted average gene expression profile). Red in heatmaps indicates greater adjacency (greater positive pairwise correlation between consensus modules). (d) Mean preservation of adjacency for all eigengenes which indicates the degree of similarity in module co-expression correlation patterns. More consistently red columns in panel (e) equate to higher values for each module in panel (d). (e) Preservation of the network between *Chrysemys* and *Apalone*. More intense red indicates greater preservation, and thus greater similarity of the modules between species. Note that module colors in this figure correspond to consensus modules in Figure 7.

from *Apalone*, *Chrysemys* is as appropriate a proxy as any other TSD cryptodiran (Bista et al., 2021), recognizing that some evolution has accrued in both lineages.

4.1 | Genome-wide gene expression patterns diverge by temperature in both *Apalone* and *Chrysemys*

To our knowledge, ours is the first application of trajectory analysis to a time series of genome-wide developmental transcriptomes, which illuminated broad patterns of gene expression underlying sexual development for both turtle species. The *Chrysemys* trajectories showed significant overall differences between temperatures, as expected given its TSD mechanism, and underscoring the power of this method to capture and quantify hyperdimensional transcriptomic patterns. Notably, 31°C elicited greater change in gene expression in *Chrysemys* than 26°C (trajectories differed in magnitude), providing a molecular explanation for why warmer temperatures in *Chrysemys* and other TSDIa turtles have greater potency to feminize embryos than the masculinizing potency of colder temperatures (Georges, 1989; Valenzuela et al., 2019). By contrast, all trajectories for *Apalone* differed in direction and shape, but never in magnitude, indicating that the total amount of change in gene expression was canalized, and that instead, different genes changed expression by temperature or by sex, and did so in a distinct manner through time in this GSD turtle.

Importantly, the trajectories began diverging between temperatures as early as stage 12 in *Chrysemys* (Figure 2C), indicating that differential expression of sex-related candidate genes in TSD turtles as early as stages 9 and 12 reflect genome-wide responses, and supporting the notion that temperatures experienced before the canonical TSP may influence sex ratios to some degree (Czerwinski et al., 2016; Gómez-Saldarriaga et al., 2016; Radhakrishnan et al., 2017, 2018; Valenzuela, 2001, 2008a, 2008b, 2010; Valenzuela et al., 2006, 2013; Valenzuela & Shikano, 2007). A remarkable difference between species was detected at stage 15, when differential expression accentuated in *Chrysemys* whereas *Apalone* trajectories remained parallel (Figure 2). This is significant, because no broad differences in the sequence or overall timing of gonadogenesis events were detected between *Apalone* and TSD turtles previously (Greenbaum & Carr, 2001), such that our data expose the conspicuous canalization in *Apalone* at the stage that marks the onset of the TSP in *Chrysemys*. Indeed, as transcriptional patterns became more

complex in *Chrysemys*, pattern of expression in *Apalone* remained impervious to the interaction effect of sex-by-temperature.

The most striking differences among trajectories within and between species occurred during the mid- and late-TSP in *Chrysemys* (Figure 2e,f), also revealing extensive thermal plasticity in genome-wide transcription in *Apalone*. Specifically, differential gene expression increased in *Chrysemys* and sex-by-temperature interactions became more complex in *Apalone*. Intriguingly, the diverging trajectory paths observed in stage 19 gonads in both taxa, lessened at stage 22 in *Chrysemys*, and between male and female *Apalone* under 26°C (Figure 2), whereas they were exacerbated between the sexes at 31°C in *Apalone*. This may suggest that sexually dimorphic genome-wide expression is less critical by the end of the TSP in the developing gonads of *Chrysemys*, and that the ancestral feminizing effect of warm temperatures (revealed by the greater magnitude of female trajectories in *Chrysemys*—see above) may be counteracted in *Apalone* by exaggerated sexually dimorphic transcription.

Using WGCNA we detected shifts in co-expression patterns of gene modules between *Apalone* and *Chrysemys* during female and male embryogenesis, some reflecting their distinct mechanisms of sexual development and perhaps driven by positive selection, while others may, in part, be indicative of developmental systems drift (True & Haag, 2001). Overall, the WGCNA analysis uncovered groups of genes within modules that were co-expressed similarly in both species, but whose relationship to other groups of genes (their correlated expression) was modified between species during their 161 My of independent evolution. The module hub genes identified in this analysis (Table 4) represent new gene candidates of interest for sexual development. Among these, *Hmgb1* is a stress response gene (Yu et al., 2015), and *Ndrg1* is associated with hormone and stress responses and may play a role in follicular development in humans (Nishigaki et al., 2022), whereas *Smca5* and *Piwil4* are involved in epigenetic regulation, and thus, plausible mediators of plasticity.

4.2 | What genes canalized softshell turtle sexual development?

Comparing the expression of several gene candidates between species suggest potential mechanistic explanations for the evolution of their contrasting sex determination, which will require future testing. In *Apalone* embryos, *Sox9*, *Aromatase*, and *Dmrt1* all showed sex-specific expression at stage 19 irrespective of temperature, as did *Sox9* at stage 22 (whereas *Aromatase* and *Dmrt1* only displayed

this pattern at 31°C at this stage) (Figure 5), such that these genes were supported as core components of the gonadal differentiation cascade as in other turtles and vertebrates (Capel, 2017; Ge et al., 2017; Morrish & Sinclair, 2002; Radhakrishnan et al., 2017; Smith et al., 2009; Valenzuela, 2008a, 2008b, 2010; Valenzuela et al., 2013; Valenzuela & Shikano, 2007). Interestingly, the up-regulation in _Apalone_ of _Sox9_ (a testis-development gene) at 31°C compared to 26°C in stage 19 males may have evolved to counter the feminizing effect that 31°C had in their TSD ancestor. By contrast, _Sox9_ and _Dmrt1_ (another testis-development gene) were thermo-insensitive in _Apalone_ females at stage 19, perhaps because the signal from the ZW genotype canalizes their transcription. Yet, at stage 22, _Sox9_ and _Dmrt1_ were upregulated in females at 26°C, the ancestral TSD expression pattern for these male-development genes. On the contrary, _Aromatase_ (a female-development gene) was upregulated at 31°C in _Apalone_ females, the typical pattern observed in _Chrysemys_ and other TSD turtles (Czerwinski et al., 2016; Radhakrishnan et al., 2017; Valenzuela & Shikano, 2007). By contrast, _Aromatase_ was mostly thermo-insensitive in _Apalone_ males (significantly upregulated but with low fold change at 26°C during stage 22), as if the two Z chromosomes of males are needed to canalize its transcription or to downregulate it below the threshold that would induce ovarian development (Figure 5). The onset of _Aromatase_ differential expression occurred earlier in _Apalone_ than in _Chrysemys_ (Figure 5), similar to the earlier expression of sexually dimorphic traits observed in other GSD vertebrates (Gross et al., 2017; Valenzuela, 2008; Valenzuela et al., 2003), and which might cause (or be the result of) the earlier commitment of gonads of GSD reptiles to their sexual fate than in their TSD close relatives (Greenbaum & Carr, 2001; Neaves et al., 2006). Additionally, _Dmrt1_ at stage 19 in _Apalone_ showed no thermal plasticity, and the onset of its canalized sex-specific transcription is conserved with _Chrysemys_, underscoring the _Dmrt1_'s central role in sexual development in turtles. Yet, _Dmrt1_ differential expression occurs earlier (in early TSP) in _Trachemys_ (Ge et al., 2017) than in _Apalone_ and _Chrysemys_ [see also (Mizoguchi & Valenzuela, 2020)], suggesting that _Dmrt1_ may be more important for male differentiation than for sex determination, consistent also with its autosomal location in _Apalone_ and its trionychid relative _Pelodiscus_ (Lee et al., 2019).

Significant changes were detected in the transcription of _Sf1_, _Wt1_, _Gata4_, and _Dax1_ in _Apalone_ compared with the TSD pattern seen in _Chrysemys_. In humans, _Sox9_ works with _Sf1_, _Wt1_, and _Gata4_ to regulate _Amh_ expression, among which _Sox9_ may be most critical (Marshall & Harley, 2000). The expression patterns of these genes observed here in _Chrysemys_ agreed with this model, showing upregulation at MPT (26°C) during the TSP. In _Apalone_, however, only _Sox9_ and _Amh_ are upregulated in males in late development (stages 19 and 22—the mid- and late-TSP of _Chrysemys_), suggesting that the genes with a lesser role no longer cooperate to regulate _Amh_, and supporting _Sox9_ as most critical for this function (Marshall & Harley, 2000). In fact, _Wt1_ and _Sf1_ were upregulated in _Apalone_ females at this point, and _Gata4_ expression was sexually monomorphic. Also in agreement, _Dax1_, a positive regulator of _Sox9_ and inhibitor

of _Sf1_, but which may induce testicular development (Ludbrook & Harley, 2004), showed no differential expression by temperature or sex in _Apalone_, suggesting that _Dax1_ may no longer regulate these two genes in this GSD turtle. It is worth noting that _Sf1_ translocated to the ZW sex chromosomes in _Apalone_ (Lee et al., 2019) within a region expanded in the W sex chromosome that was invaded by R2 retrotransposons, which affect the expression of nearby genes (Montiel et al., 2022). But whether _Sf1_ took over as a master switch gene remains untested. A hypothesis is that _Sf1's_ putative expansion on the W chromosome could have altered how these genes regulate _Amh_ during the TSP-equivalent stages, particularly because _Sf1_ was not upregulated at 26°C in _Apalone_ as it is in _Chrysemys_, and _Sf1_ is a downstream target of _Wt1_, which was upregulated at 26°C during stages 19 and 22 (as was _Gata4_ at stage 22). This would render _Wt1's_ thermosensitivity moot for sex determination. We note that _Wt1_ tended to be upregulated at 26°C during stages 12–15 in _Apalone spinifera_ as in its congener _A. mutica_ (Valenzuela, 2008b), and within males at stages 19–22 (though expression in females was even higher at these two stages). Such upregulation at cool temperatures matches the pattern in _Chrysemys_ and thus appears relic in the softshell turtle lineage (Valenzuela, 2008b). But the significance of upregulation of _Wt1_ in females observed at stages 19–22 in _Apalone_ is obscure given the clear role of _Wt1_ for testicular development in vertebrates and the lack of _Wt1_ upregulation in females across disparate taxonomic orders (Morrish & Sinclair, 2002; Valenzuela et al., 2013). Perhaps _Wt1_ regulatory role was lost in _Apalone_ or shifted to female-development, a major potential evolutionary overhaul that warrants further investigation.

Notably, given the level of thermosensitive transcription observed in _Apalone_, a counter-mechanism (presumably governed by the sex chromosomes) must exist to prevent sex ratios from being altered by temperature, which was confirmed by incubation experiments (Bull & Vogt, 1979; Ewert & Nelson, 1991). Consistently, very few genes exhibited both sex-specific thermo-insensitive expression in _Apalone_ and differential expression by temperature in _Chrysemys_ early in development (stages 9–15). Of the genes that lost thermosensitive expression in _Apalone_ compared with _Chrysemys_, _Sc5a1_, _Msi1h_, and _Ppil2_ are located on the sex chromosomes in _Apalone_ (Bista et al., 2021). Furthermore, _Sc5a1_ is a sodium-dependent glucose transporter (Turk et al., 1994), which may be relevant given the potential for calcium to help regulate TSD (Castelli et al., 2020). Furthermore, _Rrp8_ is an intriguing candidate upregulated in _Apalone_ males at stage 9, involved in chromatin remodeling (He et al., 2019) and ribosomal DNA silencing (Murayama et al., 2008), which is relevant given the contrasting epigenetic machinery transcription between _Chrysemys_ and _Apalone_ (Radhakrishnan et al., 2018).

In _Pelodiscus sinensis_, the Chinese softshell turtle that shares a homologous sex chromosome system with _Apalone_ (Badenhorst et al., 2013; Rovatsos et al., 2017), experimental overexpression of _Amh_ masculinized female embryos while its silencing feminized male embryos (Zhou et al., 2019). _Amh_ was upregulated in _Apalone_ males at stage 19 (irrespective of temperature) and at stage 22 under 31°C (Fig. 6), perhaps countering the feminizing effect of

warm temperatures and thus having a male-canalizing effect. The additional 31°C-biased thermosensitive *Amh* expression at stage 19 observed in males may help masculinize ZZ individuals incubated at ancestrally feminizing temperatures. Meanwhile, the loss of detectable thermosensitivity of *Amh* in males at stage 22 suggests a key role of *Amh* in male differentiation via thermally canalized transcription (not in sex determination, given *Amh*'s late expression, later than in *Pelodiscus*). Furthermore, *Amh*'s autosomal location (Bista et al., 2021) rules it out as a master sex-determining gene in *Apalone*. On the contrary, the ancestrally masculinizing effect of *Amh* upregulation at 26°C in females at stage 22 appears to be overridden by a feminizing factor(s) in genotypic females (we hypothesize that this may be accomplished by a W-linked factor, or a dose-dependent Z-linked factor).

Thus, our results suggest that despite the evolution of sex chromosomes in *Apalone*'s lineage, embryos need to counter the effects of relic thermosensitivity for proper sexual development, revealing a more complex interplay between residual (and novel) thermosensitivity (i.e., transcriptional plasticity) and genotypic sex determination (i.e., developmental canalization) than previously anticipated. It is interesting that we observe this pattern particularly in genes regulating the development of males (*Amh*, *Sox9*, *Dmrt1*), who are the homogametic (ZZ) sex in this species (Badenhorst et al., 2013). This suggests that two Z chromosomes may not suffice for male sex determination in *Apalone*, as observed in birds (Smith et al., 2009), and leads to the hypothesis that the W chromosome contains a/the sex-determining factor in *Apalone* rather than sex being determined by a Z-linked dosage system.

4.3 | New and old candidates for sex determination emerge, informing models of temperature-dependent sex determination

We also compared our results to recent models of TSD. In *Trachemys scripta* (Weber et al., 2020) (referred to as *Trachemys* hereafter), an increase in calcium at FPT (possibly linked to TRP proteins) causes phosphorylation of STAT3 which binds to *Kdm6b* (a positive regulator of *Dmrt1*), inhibiting its expression and that of *Dmrt1*. Importantly, protein activity of TRPV4 and phosphorylation status of STAT3 appear more critical than transcription and protein levels (Weber et al., 2020). Consistently, *Trpv4* expression in *Chrysemys* was monomorphic in our study, such that TRPV4 may play a sentinel role with monomorphic transcription adequate to respond to the environmental cue, as observed in other systems (Mateus et al., 2014). Unlike in *Trachemys* (Weber et al., 2020), *Stat3* in *Chrysemys* was upregulated at FPT (marginally at stages 9 and 15, and significantly at stage 19), whereas *Kdm6b* was upregulated at MPT at stages 9 and 19 but at FPT at stage 15, instead of steadily at MPT as in *Trachemys* (Ge et al., 2018). This suggests that KDM6B may be a less important regulator of *Dmrt1* in *Chrysemys*, consistent with *Dmrt1*'s strong upregulation in males during mid- and late TSP [this study and qPCR analyses (Mizoguchi & Valenzuela, 2020)], indicating that *Dmrt1*

plays a role in male sex differentiation but not sex determination in *Chrysemys*, counter to that proposed for *Trachemys* (Ge et al., 2017). Together, these observations strongly support the hypothesis that developmental systems drift has occurred between these two closely related emydids (Mizoguchi & Valenzuela, 2020).

Of the stress response genes potentially involved in TSD (Straková et al., 2020), only *Atp2a2* was male-upregulated across stages 9–15 in *Apalone* (Table S15). But other genes were upregulated at 26°C in stage 19–22 gonads, including *Atp2a2* and *Ano1* [both implicated in calcium transport or levels (Lytton & Maclennan, 1988; Yang et al., 2008)], genes linked to the regulation of steroids and hormones and implicated in sexual development [*Ppargc1a*, *Sst*, *Tgfb1i1* (Fujimoto et al., 1999; Patel, 1999; Tcherepanova et al., 2000)], and *Fosl2* which is involved in the formation of AP-1 (Hess et al., 2004), a transcription factor complex that interacts with SF1 (NR5A1) (Dubé et al., 2009). Interestingly, all stress-related DEGs in *Chrysemys* were both differentially expressed by sex and by temperature at some stage in *Apalone*.

Another candidate, *Cirbp*, was proposed as an activator of STAT3 given its connection to calcium and TRPV4 signaling (Weber et al., 2020). *Cirbp* shows temperature-dependent allele specific expression correlated with sex ratios in *Chelydra serpentina* (Schroeder et al., 2016), where one of two alleles is thermosensitive, and its expression is correlated with female-biased clutches. Here, we also observe upregulation at FPT of two *Cirbp* isoforms across stages in *Chrysemys* (a third rare isoform exhibited monomorphic expression). Intriguingly, three *Cirbp* isoforms were observed in *Apalone* and lacked sex-specific expression but were always upregulated at 31°C in both sexes, perhaps reflecting a stress response (Liao et al., 2017) to constant warm temperatures but with no role on sexual development in *Apalone*, as may also occur in *Chrysemys*. It should be noted that *Cirbp*'s association with femaleness remains tenuous, because the expression of the allele associated with male-biased clutches in *C. serpentina* (Schroeder et al., 2016) was not thermosensitive, rather carrying that allele was associated with maleness, whereas carrying the alternate allele was associated both with temperature and femaleness, such that its role could not be detangled in that study.

The model by Weber and collaborators (Weber et al., 2020) fits well with the CaRe (cellular Calcium and Redox) status hypothesis (Castelli et al., 2020), and proposes that pathways related to stress and calcium signaling could be co-opted for the evolution of TSD. Here, we detected monomorphic expression of many stress-related genes in both species, ruling them out for a dual role in sexual development. Interestingly, data from later stages in *Apalone* (and not *Chrysemys*) suggest a possible relationship between sex and stress, but experiments detangling sex and temperature are needed to test whether the same may occur in *Chrysemys*. *Atp2a2* is particularly intriguing because it is related to calcium transport (Lytton & Maclennan, 1988), was a DEG at stages 15–19 in *Chrysemys* (onset and mid TSP), and at least one transcript was differentially expressed by sex at every stage in *Apalone* and by temperature for stages 9, 12, and 19. Finding stress-response genes with sustained upregulation at warmer temperatures in *Chrysemys* is particularly important

to elucidate the molecular architecture underlying increased feminization and mortality predicted for this and many TSD turtles under climate change (Jensen et al., 2020; Valenzuela et al., 2019).

5 | CONCLUSIONS

Our unprecedented trajectory analysis of transcriptomic time series from sexed embryos of a GSD reptile incubated under temperatures that induce maleness and femaleness ancestrally, illuminated the evolution of sexual development in a turtle with sex chromosomes. We found that extensive plasticity in transcription persists over millions of years after developmental canalization evolves, eliciting active transcriptional countermeasures to prevent phenotypic and genotypic mismatch. Our findings inform our understanding of how environmental cues might be translated into molecular signals for development by (a) identifying new and validating well-known members of the vertebrate sexual development network, (b) identifying novel sex-determining candidate genes in a ZZ/ZW turtle, (c) strengthening the hypothesis that stress and sexual development might be associated, and (d) highlighting evolutionary remodeling of transcriptional patterns that accompanied the transition from plasticity to canalization.

Several inferences follow our results:

1. The evolution of canalization does not require genome-wide environmental insensitivity.
2. Lingering thermosensitivity may be neutral to natural selection and co-optable for the evolutionary reversal from GSD to TSD, or for other thermal adaptation.
3. Climate change may alter gene expression in GSD turtles (not just TSD taxa), potentially triggering increased canalization in sexual development (i.e., genetic assimilation) or a turnover of sex determination.

DATA AVAILABILITY STATEMENT

All sequencing reads and gene expression data are deposited in the Short Read Archive at NCBI: BioProjects PRJNA683586 (*Apalone spinifera* embryos—SRR13224849-SRR13224888) and PRJNA594037 (*Chrysemys picta* embryos—study number SRP237291; SRR10674595-SRR10674614). *Apalone spinifera* genome assembly is available at NCBI (BioProject: PRJNA837702).

BENEFIT SHARING

Research benefits will result from the sharing of these datasets on public databases as described in the Data Accessibility section.

ORCID

Thea B. Gessler https://orcid.org/0000-0002-0701-0389
Zhiqiang Wu https://orcid.org/0000-0002-4238-7317
Nicole Valenzuela https://orcid.org/0000-0003-1148-631X

REFERENCES

Abreu-Grobois, F. A., Morales-Mérida, B. A., Hart, C. E., Guillon, J.-M., Godfrey, M. H., Navarro, E., & Girondot, M. (2020). Recent advances on the estimation of the thermal raction norm for sex ratios. *PeerJ*, *8*, e8451. https://doi.org/10.7717/peerj.8451

Adams, D., & Collyer, M. (2009). A general framework for the analysis of phenotypic trajectories in evolutionary studies. *Evolution*, *63*(5), 1143–1154. https://doi.org/10.1111/j.1558-5646.2009.00649.x

Ashburner, M., Ball, C., Blake, J., Botstein, D., Butler, H., Cherry, J., Davis, A. P., Dolinski, K., Dwight, S. S., Eppig, J. T., Harris, M. A., Hill, D. P., Issel-Tarver, L., Kasarskis, A., Lewis, S., Matese, J. C., Richardson, J. E., Ringwald, M., Rubin, G. M., & Sherlock, G. (2000). Gene ontology: Tool for the unification of biology. *Nature Genetics*, *25*(1), 25–29. https://doi.org/10.1038/75556

Bachtrog, D., Kirkpatrick, M., Mank, J. E., McDaniel, S. F., Pires, J. C., Rice, W., & Valenzuela, N. (2011). Are all sex chromosomes created equal? *Trends in Genetics*, *27*(9), 350–357. http://linkinghub.elsevier.com/retrieve/pii/S0168952511000667

Bachtrog, D., Mank, J., Peichel, C., Kirkpatrick, M., Otto, S., Ashman, T., Hahn, M. W., Kitano, J., Mayrose, I., Ming, R., Perrin, N., Ross, L., Valenzuela, N., Vamosi, J. C., & Tree of Sex Consortium. (2014). Sex determination: Why so many ways of doing it? *PLoS Biology*, *12*(7), e1001899. https://doi.org/10.1371/journal.pbio.1001899

Badenhorst, D., Hillier, L., Literman, R., Montiel, E., Radhakrishnan, S., Shen, Y., Minx, P., Janes, D. E., Warren, W. C., Edwards, S. V., & Valenzuela, N. (2015). Physical mapping and refinement of the painted turtle genome (Chrysemys picta) inform amniote genome evolution and challenge turtle-bird chromosomal conservation. *Genome Biology and Evolution*, *7*(7), 2038–2050. https://doi.org/10.1093/gbe/evv119

Badenhorst, D., Stanyon, R., Engstrom, T., & Valenzuela, N. (2013). A ZZ/ZW microchromosome system in the spiny softshell turtle, Apalone spinifera, reveals an intriguing sex chromosome conservation in Trionychidae. *Chromosome Research*, *21*(2), 137–147. https://doi.org/10.1007/s10577-013-9343-2

Bauer, S., Gagneur, J., & Robinson, P. (2010). GOing Bayesian: Model-based gene set analysis of genome-scale data. *Nucleic Acids Research*, *38*(11), 3523–3532. https://doi.org/10.1093/nar/gkq045

Bauer, S., Grossmann, S., Vingron, M., & Robinson, P. (2008). Ontologizer 2.0—A multifunctional tool for GO term enrichment analysis and data exploration. *Bioinformatics*, *24*(14), 1650–1651. https://doi.org/10.1093/bioinformatics/btn250

Beldade, P., Mateus, A., & Keller, R. (2011). Evolution and molecular mechanisms of adaptive developmental plasticity. *Molecular Ecology*, *20*(7), 1347–1363. https://doi.org/10.1111/j.1365-294X.2011.05016.x

Bista, B., & Valenzuela, N. (2020). Turtle insights into the evolution of the reptilian karyotype and the genomic architecture of sex determination [review]. *Genes*, *11*(4), 416. https://doi.org/10.3390/genes11040416

Bista, B., Wu, Z., Literman, R., & Valenzuela, N. (2021). Thermosensitive sex chromosome dosage compensation in ZZ/ZW softshell turtles, Apalone spinifera. *Philosophical Transactions of the Royal Society B-Biological Sciences*, *376*(1833), 20200101. https://doi.org/10.1098/rstb.2020.0101

Bolger, A., Lohse, M., & Usadel, B. (2014). Trimmomatic: A flexible trimmer for Illumina sequence data. *Bioinformatics*, *30*(15), 2114–2120. https://doi.org/10.1093/bioinformatics/btu170

Bray, N., Pimentel, H., Melsted, P., & Pachter, L. (2016). Near-optimal probabilistic RNA-seq quantification. *Nature Biotechnology*, *34*(5), 525–527. https://doi.org/10.1038/nbt.3519

Bull, J. (1983). *Evolution of sex determining mechanisms*. Benjamin/Cummings Publ. Co.

Bull, J., & Vogt, R. (1979). Temperature-dependent sex determination in turtles. *Science*, *206*(4423), 1186–1188. https://doi.org/10.1126/science.505003

Bull, J., & Vogt, R. (1981). Temperature-sensitive periods of sex determination in Emydid turtles. *The Journal of Experimental Zoology*, *218*(3), 435–440. https://doi.org/10.1002/jez.1402180315

Camacho, C., Coulouris, G., Avagyan, V., Ma, N., Papadopoulos, J., Bealer, K., & Madden, T. (2009). BLAST+: Architecture and applications. *BMC Bioinformatics*, *10*, 1–9. https://doi.org/10.1186/1471-2105-10-421

Capel, B. (2017). Vertebrate sex determination: Evolutionary plasticity of a fundamental switch. *Nature Reviews Genetics*, *18*(11), 675–689. https://doi.org/10.1038/nrg.2017.60

Castelli, M., Whiteley, S., Georges, A., & Holleley, C. (2020). Cellular calcium and redox regulation: The mediator of vertebrate environmental sex determination? *Biological Reviews*, *95*(3), 680–695. https://doi.org/10.1111/brv.12582

Chen, H. (2018). VennDiagram: Generate high-resolution venn and euler plots. In (Version 1.6.20) https://CRAN.R-project.org/package=VennDiagram

Collyer, M., & Adams, D. (2007). Analysis of two-state multivariate phenotypic change in ecological studies. *Ecology*, *88*(3), 683–692. https://doi.org/10.1890/06-0727

Collyer, M., & Adams, D. (2013). Phenotypic trajectory analysis: Comparison of shape change patterns in evolution and ecology. *Hystrix the Italian Journal of Mammalogy*, *24*(1), 75–83. https://doi.org/10.4404/hystrix-24.1-6298

Collyer, M., & Adams, D. (2018). RRPP: An r package for fitting linear models to high-dimensional data using residual randomization. *Methods in Ecology and Evolution*, *9*(7), 1772–1779. https://doi.org/10.1111/2041-210X.13029

Czerwinski, M., Natarajan, A., Barske, L., Looger, L., & Capel, B. (2016). A timecourse analysis of systemic and gonadal effects of temperature on sexual development of the red-eared slider turtle Trachemys scripta elegans. *Developmental Biology*, *420*(1), 166–177. https://doi.org/10.1016/j.ydbio.2016.09.018

Dubé, C., Bergeron, F., Vaillant, M.-J., Robert, N., Brousseau, C., & Tremblay, J. (2009). The nuclear receptors SF1 and LRH1 are expressed in endometrial cancer cells and regulate steroidogenic gene transcription by cooperating with AP-1 factors. *Cancer Letters*, *275*, 127–138. https://doi.org/10.1016/j.canlet.2008.10.008

Ewert, M., Etchberger, C., & Nelson, C. (2004). Turtle sex-determining modes and TSD patterns, and some TSD pattern correlates. In N. Valenzuela & V. Lance (Eds.), *Temperature Dependent Sex Determination in Vertebrates* (pp. 21–32). Smithsonian Books.

Ewert, M. A., & Nelson, C. E. (1991). Sex determination in turtles: Diverse patterns and some possible adaptive values. *Copeia*, *1991*(1), 50. https://doi.org/10.2307/1446248

Fu, L., Niu, B., Zhu, Z., Wu, S., & Li, W. (2012). CD-HIT: Accelerated for clustering the next-generation sequencing data. *Bioinformatics*, *28*(23), 3150–3152. https://doi.org/10.1093/bioinformatics/bts565

Fujimoto, N., Yeh, S., Kang, H.-Y., Inui, S., Chang, H.-C., Mizokami, A., & Chang, C. (1999). Cloning and characterization of androgen receptor coactivator, ARA55, in human prostate. *Journal of Biological Chemistry*, *274*(12), 8316–8321. https://doi.org/10.1074/jbc.274.12.8316

Ge, C., Ye, J., Weber, C., Sun, W., Zhang, H., Zhou, Y., Cai, C., Qian, G., & Capel, B. (2018). The histone demethylase KDM6B regulates temperature-dependent sex determination in a turtle species. *Science*, *360*(6389), 645–648. https://doi.org/10.1126/science.aap8328

Ge, C., Ye, J., Zhang, H., Zhang, Y., Sun, W., Sang, Y., Capel, B., & Qian, G. (2017a). Dmrt1 induces the male pathway in a turtle species with temperature-dependent sex determination. *Development*, *144*(12), 2222–2233. https://doi.org/10.1242/dev.152033

Georges, A. (1989). Female turtles from hot nests: Is it duration of incubation or proportion of development at high temperatures that matters? *Oecologia*, *81*(3), 323–328. https://doi.org/10.1007/BF00377078

Gomez-Mestre, I., & Buchholz, D. (2006). Developmental plasticity mirrors differences among taxa in spadefoot toads linking plasticity and diversity. *Proceedings of the National Academy of Sciences*, *103*, 19021–19026. https://doi.org/10.1073/pnas.0603562103

Gómez-Saldarriaga, C., Valenzuela, N., & Ceballos, C. (2016). Effects of incubation temperature on sex determination in the endangered magdalena river turtle, Podocnemis lewyana [text]. *Chelonian Conservation Biology*, *15*(1), 43–53. https://doi.org/10.2744/CCB-1170.1

Grabherr, M., Haas, B., Yassour, M., Levin, J., Thompson, D., Amit, I., Adiconis, X., Fan, L., Raychowdhury, R., Zeng, Q., Chen, Z., Mauceli, E., Hacohen, N., Gnirke, A., Rhind, N., di Palma, F., Birren, B. W., Nusbaum, C., Lindblad-Toh, K., … Regev, A. (2011). Full-length transcriptome assembly from RNA-seq data without a reference genome. *Nature Biotechnology*, *29*(7), 644–652. https://doi.org/10.1038/nbt.1883

Greenbaum, E., & Carr, J. (2001). Sexual differentiation in the spiny softshell turtle (Apalone spinifera), a species with genetic sex determination. *The Journal of Experimental Zoology*, *290*(2), 190–200. https://doi.org/10.1002/jez.1049

Greenbaum, E., & Carr, J. L. (2002). Staging criteria for embryos of the spiny softshell turtle, *Apalone spinifera* (testudines: Trionychidae). *Journal of Morphology*, *254*(3), 272–291. https://doi.org/10.1002/jmor.10036

Gross, N., Kropp, J., & Khatib, H. (2017). Sexual dimorphism of miRNAs secreted by bovine in vitro-produced embryos. *Frontiers in Genetics*, *8*, 39. https://doi.org/10.3389/fgene.2017.00039

Gutzke, W. H., Packard, G. C., Packard, M., & Boardman, T. J. (1987). Influence of the hydric and thermal environments on eggs and hatchlings of painted turtles (*Chrysemys picta*). *Herpetologica*, *43*(4), 393–404. https://doi.org/10.2307/3892142

Hammes, A., Guo, J.-K., Lutsch, G., Leheste, J.-R., Landrock, D., Ziegler, U., Gubler, M. C., & Schedl, A. (2001). Two splice variants of the Wilms' tumor 1 gene have distinct functions during sex determination and nephron formation. *Cell*, *106*(3), 319–329. https://doi.org/10.1016/s0092-8674(01)00453-6

He, J., Fu, X., Zhang, M., He, F., Li, W., Abdul, M., Zhou, J., Sun, L., Chang, C., Li, Y., Liu, H., Wu, K., Babarinde, I. A., Zhuang, Q., Loh, Y. H., Chen, J., Esteban, M. A., & Hutchins, A. P. (2019). Transposable elements are regulated by context-specific patterns of chromatin

marks in mouse embryonic stem cells. *Nature Communications*, *10*(1), 34. https://doi.org/10.1038/s41467-018-08006-y

Hess, J., Angel, P., & Schorpp-Kistner, M. (2004). AP-1 subunits: Quarrel and harmony among siblings. *Journal of Cell Science*, *117*(25), 5965–5973. https://doi.org/10.1242/jcs.01589

Huang, X., Chen, X.-G., & Armbruster, P. (2016). Comparative performance of transcriptome assembly methods for non-model organisms [OriginalPaper]. *BMC Genomics*, *17*(1), 1–14. https://doi.org/10.1186/s12864-016-2923-8

Janzen, F., & Krenz, J. (2004). Phylogenetics: Which was first, TSD or GSD? In N. Valenzuela & V. Lance (Eds.), *Temperature dependent sex determination in vertebrates* (pp. 121–130). Smithsonian. https://lib.dr.iastate.edu/cgi/viewcontent.cgi?article=1166&context=eeob_ag_pubs, https://lib.dr.iastate.edu/eeob_ag_pubs/167

Jensen, M., Allen, C., Eguchi, T., Bell, I., LaCasella, E., Hilton, W., Hof, C. A. M., & Dutton, P. H. (2020). Environmental warming and feminization of one of the largest sea turtle populations in the world. *Current Biology*, *28*(1), 154–159. https://doi.org/10.1016/j.cub.2017.11.057

Kratochvíl, L., Stöck, M., Rovatsos, M., Bullejos, M., Herpin, A., Jeffries, D. L., Peichel, C. L., Perrin, N., Valenzuela, N., & Pokorná, M. J. (2021). Expanding the classical paradigm: What we have learnt from vertebrates about sex chromosome evolution. *Philosophical Transactions of the Royal Society B: Biological Sciences*, *376*(1833), 20200097. https://doi.org/10.1098/rstb.2020.0097

Langfelder, P., & Horvath, S. (2008). WGCNA: An R package for weighted correlation network analysis [OriginalPaper]. *BMC Bioinformatics*, *9*(1), 1–13. https://doi.org/10.1186/1471-2105-9-559

Lee, L., Montiel, E., Navarro-Domínguez, B., & Valenzuela, N. (2019). Chromosomal rearrangements during turtle evolution altered the synteny of genes involved in vertebrate sex determination. *Cytogenetic and Genome Research*, *157*(1–2), 77–88. https://doi.org/10.1159/000497302

Li, H. (2011). A statistical framework for SNP calling, mutation discovery, association mapping and population genetical parameter estimation from sequencing data. *Bioinformatics*, *27*(21), 2987–2993. https://doi.org/10.1093/bioinformatics/btr509

Li, H., Handsaker, B., Wysoker, A., Fennell, T., Ruan, J., Homer, N., Marth, G., Abecasis, G., Durbin, R., & 1000 Genome Project Data Processing Subgroup. (2009). The sequence alignment/map format and SAMtools. *Bioinformatics*, *25*(16), 2078–2079. https://doi.org/10.1093/bioinformatics/btp352

Li, W., & Godzik, A. (2006). CD-HIT: A fast program for clustering and comparing large sets of protein or nucleotide sequences. *Bioinformatics*, *22*(13), 1658–1659. https://doi.org/10.1093/bioinformatics/btl158

Liao, Y., Tong, L., Tang, L., & Wu, S. (2017). The role of cold-inducible RNA binding protein in cell stress response. *International Journal of Cancer*, *141*(11), 2164–2173. https://doi.org/10.1002/ijc.30833

Literman, R., Badenhorst, D., & Valenzuela, N. (2014). qPCR-based molecular sexing by copy number variation in rRNA genes and its utility for sex identification in soft-shell turtles. *Methods in Ecology and Evolution*, *5*, 872–880. https://doi.org/10.1111/2041-210X.12228

Literman, R., Burrett, A., Bista, B., & Valenzuela, N. (2018). Putative independent evolutionary reversals from genotypic to temperature-dependent sex determination are associated with accelerated evolution of sex-determining genes in turtles. *Journal of Molecular Evolution*, *86*(1), 11–26. https://doi.org/10.1007/s00239-017-9820-x

Literman, R., Radhakrishnan, S., Tamplin, J., Burke, R., Dresser, C., & Valenzuela, N. (2017). Development of sexing primers in Glyptemys insculpta and Apalone spinifera turtles uncovers an XX/XY sex-determining system in the critically-endangered bog turtle Glyptemys muhlenbergii [OriginalPaper]. *Conservation Genetics Resources*, *9*(4), 651–658. https://doi.org/10.1007/s12686-017-0711-7

Liu, M., Adelman, Z., Myles, K., & Zhang, L. (2014). A transcriptome post-scaffolding method for assembling high quality contigs [research article]. *Computational Biology Journal*, *2014*, 1–4. https://doi.org/10.1155/2014/961823

Love, M., Huber, W., & Anders, S. (2014). Moderated estimation of fold change and dispersion for RNA-seq data with DESeq2 [OriginalPaper]. *Genome Biology*, *15*(12), 1–21. https://doi.org/10.1186/s13059-014-0550-8

Ludbrook, L., & Harley, V. (2004). Sex determination: A 'window' of DAX1 activity. *Trends in Endocrinology and Metabolism*, *15*(3), 116–121. https://doi.org/10.1016/j.tem.2004.02.002

Lynch, M., & Marinov, G. (2015). The bioenergetic costs of a gene. *PNAS*, *112*(51), 15690–15695. https://doi.org/10.1073/pnas.1514974112

Lytton, J., & Maclennan, D. (1988). Molecular cloning of cDNAs from human kidney coding for two alternatively spliced products of the cardiac Ca^2+-ATPase gene. *Journal of Biological Chemistry*, *263*(29), 15024–15031. https://doi.org/10.1016/s0021-9258(18)68141-4

Marshall, O., & Harley, V. (2000). Molecular mechanisms of SOX9 action. *Molecular Genetics and Metabolism*, *71*, 455–462. https://doi.org/10.1006/mgme.2000.3081

Matesanz, S., Gianoli, E., & Valladares, F. (2010). Global change and the evolution of phenotypic plasticity in plants. *Annals of the New York Academy of Science*, *1206*, 35–55. https://doi.org/10.1111/j.1749-6632.2010.05704.x

Mateus, A., Marques-Pita, M., Oostra, V., Lafuente, E., Brakefield, P., Zwaan, B., & Beldade, P. (2014). Adaptive developmental plasticity: Compartmentalized responses to environmental cues and to corresponding internal signals provide phenotypic flexibility [OriginalPaper]. *BMC Biology*, *12*(1), 1–15. https://doi.org/10.1186/s12915-014-0097-x

Merchant-Larios, H., Díaz-Hernández, V., & Cortez, D. (2021). Molecular and cellular mechanisms underlying temperature-dependent sex determination in turtles. *Sexual Development*, *15*(1–3), 38–46. https://doi.org/10.1159/000515296

Mizoguchi, B., & Valenzuela, N. (2020). Alternative splicing and thermosensitive expression of Dmrt1 during urogenital development in the painted turtle, *Chrysemys Picta*. *PeerJ*, *8*, e8639. https://doi.org/10.7717/peerj.8639

Montiel, E. E., Badenhorst, D., Lee, L., & Valenzuela, N. (2022). Evolution and dosage compensation of nucleolar organizing regions (NORs) mediated by mobile elements in turtles with female (ZZ/ZW) but not with male (XX/XY) heterogamety. *Journal of Evolutionary Biology.*, *35*, 1709–1720. https://doi.org/10.1111/jeb.14064

Morrish, B., & Sinclair, A. (2002). Vertebrate sex determination: Many means to an end. *Reproduction*, *124*(4), 447–457. https://doi.org/10.1530/rep.0.1240447

Mu, Y., Zhao, B., Tang, W.-Q., Sun, B.-J., Zeng, Z.-G., Valenzuela, N., & Du, W.-G. (2015). Temperature-dependent sex determination ruled out in the Chinese soft-shelled turtle (*Pelodiscus sinensis*) via molecular cytogenetics and incubation experiments across populations. *Sexual Development*, *9*(2), 111–117. https://doi.org/10.1159/000373903

Murayama, A., Ohmori, K., Fujimura, A., Minami, H., Yasuzawa-Tanaka, K., Kuroda, T., Oie, S., Daitoku, H., Okuwaki, M., Nagata, K., Fukamizu, A., Kimura, K., Shimizu, T., & Yanagisawa, J. (2008). Epigenetic control of rDNA loci in response to intracellular energy status. *Cell*, *133*(4), 627–639. https://doi.org/10.1016/j.cell.2008.03.030

Neaves, L., Wapstra, E., Birch, D., Girling, J., & Joss, J. (2006). Embryonic gonadal and sexual organ development in a small viviparous skink, Niveoscincus ocellatus. *Journal of Experimental Zoology Part A: Comparative Experimental Biology*, *305*(1), 74–82. https://doi.org/10.1002/jez.a.249

Nishigaki, A., Tsubokura, H., Ishida, M., Hashimoto, Y., Yoshida, A., Hisamatsu, Y., Tsuzuki-Nakao, T., Murata, H., & Okada, H. (2022). NDRG1 is expressed in human granulosa cells: An implicative role of NDRG1 in the ovary. *Reproductive Medicine and Biology*, *21*(1), e12437. https://doi.org/10.1002/rmb2.12437

Oh, V. K. S., & Li, R. B. W. (2021). Temporal dynamic methods for bulk rna-seq time series data. *Genes*, *12*(3), 352. https://doi.org/10.3390/genes12030352

Organ, C., & Janes, D. (2008). Evolution of sex chromosomes in Sauropsida. *Integrative and Comparative Biology*, *48*(4), 512–519. https://doi.org/10.1093/icb/icn041

Patel, Y. (1999). Somatostatin and its receptor family. *Frontiers in Neuroendocrinology*, *20*(3), 157–198. https://doi.org/10.1006/frne.1999.0183

R Core Development Team. (2018). *R: a language and envrionment for statistical computing*. In (Version 3.5) R Foundation for Statistical Computing. http://cran.R-project.org

Radhakrishnan, S., Literman, R., Neuwald, J., Severin, A., & Valenzuela, N. (2017). Transcriptomic responses to environmental temperature by turtles with temperature-dependent and genotypic sex determination assessed by RNAseq inform the genetic architecture of embryonic gonadal development. *PLoS One*, *12*(3), e0172044. https://doi.org/10.1371/journal.pone.0172044

Radhakrishnan, S., Literman, R., Neuwald, J., & Valenzuela, N. (2018). Thermal response of epigenetic genes informs turtle sex determination with and without sex chromosomes. *Sexual Development*, *12*, 308–319. https://doi.org/10.1159/000492188

Robinson, M., & Oshlack, A. (2010). A scaling normalization method for differential expression analysis of RNA-seq data [OriginalPaper]. *Genome Biology*, *11*(3), 1–9. https://doi.org/10.1186/gb-2010-11-3-r25

Rovatsos, M., & Kratochvíl, L. (2021). Evolution of dosage compensation does not depend on genomic background. *Molecular Ecology*, *30*(8), 1836–1845. https://doi.org/10.1111/mec.15853

Rovatsos, M., Praschag, P., Fritz, U., & Kratochvsl, L. (2017). Stable cretaceous sex chromosomes enable molecular sexing in softshell turtles (testudines: Trionychidae). *Scientific Reports*, *7*, 42150. https://doi.org/10.1038/srep42150

Sabath, N., Itescu, Y., Feldman, A., Meiri, S., Mayrose, I., & Valenzuela, N. (2016). Sex determination, longevity, and the birth and death of reptilian species. *Ecology and Evolution*, *6*(15), 5207–5220. https://doi.org/10.1002/ece3.2277

Schroeder, A., Metzger, K., Miller, A., & Rhen, T. (2016). A novel candidate gene for temperature-dependent sex determination in the common snapping turtle. *Genetics*, *203*(1), 557–571. https://doi.org/10.1534/genetics.115.182840

Schwanz, L., & Georges, A. (2021). Sexual development and the environment: Conclusions from 40 years of theory. *Sexual Development*, *15*(1-3), 7–22.

Simão, F., Waterhouse, R., Ioannidis, P., Kriventseva, E., & Zdobnov, E. (2015). BUSCO: Assessing genome assembly and annotation completeness with single-copy orthologs. *Bioinformatics*, *31*(19), 3210–3212. https://doi.org/10.1093/bioinformatics/btv351

Smith, C., Roeszler, K., Ohnesorg, T., Cummins, D., Farlie, P., Doran, T., & Sinclair, A. (2009). The avian Z-linked gene DMRT1 is required for male sex determination in the chicken. *Nature*, *461*(7261), 267–271. https://doi.org/10.1038/nature08298

Spotila, L. D., Spotila, J. R., & Hall, S. E. (1998). Sequence and expression analysis of WT1 and Sox9 in the red-eared slider turtle, *Trachemys scripta*. *The Journal of Experimental Zoology*, *281*(5), 417–427. https://doi.org/10.1002/(sici)1097-010x(19980801)281:5<417::aid-jez7>3.0.co;2-r

Stöck, M., Kratochvíl, L., Kuhl, H., Rovatsos, M., Evans, B. J., Suh, A., Valenzuela, N., Veyrunes, F., Zhou, Q., Gamble, T., Capel, B., Schartl, M., & Guiguen, Y. (2021). A brief review of vertebrate sex evolution with a pledge for integrative research: Towards ' <i>-sexomics</i> '. *Philosophical Transactions of the Royal Society B: Biological Sciences*, *376*(1832), 20200426. https://doi.org/10.1098/rstb.2020.0426

Straková, B., Rovatsos, M., Kubička, L., & Kratochvíl, L. (2020). Evolution of sex determination in amniotes: Did stress and sequential hermaphroditism produce environmental determination? *BioEssays*, *42*(10), 2000050. https://doi.org/10.1002/bies.202000050

Tcherepanova, I., Puigserver, P., Norris, J., Spiegelman, B., & Mcdonnell, D. (2000). Modulation of estrogen receptor-α transcriptional activity by the coactivator PGC-1. *Journal of Biological Chemistry*, *275*(21), 16302–16308. https://doi.org/10.1074/jbc.m001364200

The Gene Ontology Consortium. (2019). The gene ontology resource: 20 years and still GOing strong. *Nucleic Acids Research*, *47*(D1), D330–D338. https://doi.org/10.1093/nar/gky1055

The RNAcentral Consortium. (2019). RNAcentral: A hub of information for non-coding RNA sequences. *Nucleic Acids Research*, *47*(D1), D221–D229. https://doi.org/10.1093/nar/gky1034

The UniProt Consortium. (2018). UniProt: A worldwide hub of protein knowledge. *Nucleic Acids Research*, *47*(D1), D506–D515. https://doi.org/10.1093/nar/gky1049

Tokita, M., & Kuratani, S. (2001). Normal embryonic stages of the Chinese softshelled turtle Pelodiscus sinensis (Trionychidae). *Zoological Science*, *18*, 705–715. https://doi.org/10.2108/zsj.18.705.full

Tree of Sex Consortium. (2014). Tree of sex: A database of sexual systems. *Scientific Data*, *1*, 140015. https://doi.org/10.1038/sdata.2014.15

True, J., & Haag, E. (2001). Developmental system drift and flexibility in evolutionary trajectories. *Evolution & Development*, *3*(2), 109–119. https://doi.org/10.1046/j.1525-142x.2001.003002109.x

Turk, E., Martín, M., & Wright, E. (1994). Structure of the human Na+/glucose cotransporter gene SGLT1. *Journal of Biological Chemistry*, *269*(21), 15204–15209. https://doi.org/10.1016/s0021-9258(17)36592-4

Valenzuela, N. (2001). Constant, shift, and natural temperature effects on sex determination in Podocnemis expansa turtles. *Ecology*, *82*(11), 3010–3024. https://doi.org/10.1890/0012-9658(2001)082[3010:CSANTE]2.0.CO;2

Valenzuela, N. (2008). Sexual development and the evolution of sex determination. *Sexual Development*, *2*(2), 64–72.

Valenzuela, N. (2008a). Evolution of the gene network underlying gonadogenesis in turtles with temperature-dependent and genotypic sex determination. *Integrative and Comparative Biology*, *48*(4), 476–485. https://doi.org/10.1093/icb/icn031

Valenzuela, N. (2008b). Relic thermosensitive gene expression in a turtle with genotypic sex determination. *Evolution*, *62*(1), 234–240. https://doi.org/10.1111/j.1558-5646.2007.00279.x

Valenzuela, N. (2009). Egg incubation and collection of painted turtle embryos. *Cold Spring Harbor Protocols*, *2009*(7), pdb.prot5238. https://doi.org/10.1101/pdb.prot5238

Valenzuela, N. (2010). Multivariate expression analysis of the gene network underlying sexual development in turtle embryos with temperature-dependent and genotypic sex determination. *Sexual Development*, *4*(1–2), 39–49. https://doi.org/10.1159/000277935

Valenzuela, N. (2018). Causes and consequences of evolutionary transitions in the level of phenotypic plasticity of reptilian sex determinaiton. In J. Leonard (Ed.), *Transitions between sexual systems: Understanding the evolution of hermaphroditism and dioecy*. Springer Verlag.

Valenzuela, N. (2021). *Podocnemis expansa turtles hit to a unifying explanation for the evolution of temperature dependent sex determination in long-lived and short-lived vertebrates*. In press.

Valenzuela, N., & Adams, D. (2011). Chromosome number and sex determination coevolve in turtles. *Evolution*, *65*(6), 1808–1813. https://doi.org/10.1111/j.1558-5646.2011.01258.x

Valenzuela, N., Adams, D., & Janzen, F. (2003). Pattern does not equal process: Exactly when is sex environmentally determined? *The American Naturalist*, *161*(4), 676–683. https://doi.org/10.1086/368292

Valenzuela, N., Badenhorst, D., Montiel, E. E., & Literman, R. (2014). Molecular cytogenetic search for cryptic sex chromosomes in painted turtles *Chrysemys picta*. *Cytogenetic and Genome Research*, *144*(1), 39–46. https://doi.org/10.1159/000366076

Valenzuela, N., LeClere, A., & Shikano, T. (2006). Comparative gene expression of steroidogenic factor 1 in *Chrysemys picta* and *Apalone mutica* turtles with temperature-dependent and genotypic sex determination. *Evolution and Development*, 8(5), 424–432. https://doi.org/10.1111/j.1525-142X.2006.00116.x

Valenzuela, N., Literman, N., Neuwald, J. L., Mizoguchi, B., Iverson, J. B., Riley, J. L., & Litzgus, J. D. (2019). Extreme thermal fluctuations from climate change unexpectedly accelerate demographic collapse of vertebrates with temperature-dependent sex determination. *Scientific Reports*, 9(1), 1–11. https://doi.org/10.1038/s41598-019-40597-4

Valenzuela, N., Neuwald, J., & Literman, R. (2013). Transcriptional evolution underlying vertebrate sexual development. *Developmental Dynamics*, 242(4), 307–319. https://doi.org/10.1002/dvdy.23897

Valenzuela, N., & Shikano, T. (2007). Embryological ontogeny of aromatase gene expression in Chrysemys picta and Apalone mutica turtles: Comparative patterns within and across temperature-dependent and genotypic sex-determining mechanisms. *Development Genes and Evolution*, 217(1), 55–62. https://doi.org/10.1007/s00427-006-0106-3

Weber, C., Zhou, Y., Lee, J., Looger, L., Qian, G., Ge, C., & Capel, B. (2020). Temperature-dependent sex determination is mediated by pSTAT3 repression of Kdm6b. *Science*, 368(6488), 303–306. https://doi.org/10.1126/science.aaz4165

West-Eberhard, M. J. (2003). *Developmental plasticity and evolution.* Oxford University Press.

Wu, T., & Nacu, S. (2010). Fast and SNP-tolerant detection of complex variants and splicing in short reads. *Bioinformatics*, 26(7), 873–881. https://doi.org/10.1093/bioinformatics/btq057

Wu, T., & Watanabe, C. (2005). GMAP: A genomic mapping and alignment program for mRNA and EST sequences. *Bioinformatics*, 21(9), 1859–1875. https://doi.org/10.1093/bioinformatics/bti310

Yang, Y., Cho, H., Koo, J., Tak, M., Cho, Y., Shim, W.-S., Park, S. P., Lee, J., Lee, B., Kim, B. M., Raouf, R., Shin, Y. K., & Oh, U. (2008). TMEM16A confers receptor-activated calcium-dependent chloride conductance. *Nature*, 455(7217), 1210–1215. https://doi.org/10.1038/nature07313

Yntema, C. (1968). A series of stages in the embryonic development of Chelydra serpentina. *Journal of Morphology*, 125(2), 219–251. https://doi.org/10.1002/jmor.1051250207

Yu, Y., Tang, D., & Kang, R. (2015). Oxidative stress-mediated HMGB1 biology. *Frontiers in Physiology*, 6, 93. https://doi.org/10.3389/fphys.2015.00093

Zdobnov, E., Tegenfeldt, F., Kuznetsov, D., Waterhouse, R., Simão, F., Ioannidis, P., Seppey, M., Loetscher, A., & Kriventseva, E. V. (2016). OrthoDB v9.1: Cataloging evolutionary and functional annotations for animal, fungal, plant, archaeal, bacterial and viral orthologs. *Nucleic Acids Research*, 45(D1), D744–D749. https://doi.org/10.1093/nar/gkw1119

Zhang, B., & Horvath, S. (2005). A general framework for weighted gene co-expression network analysis. *Statistical Applications in Genetics and Molecular Biology*, 4, 17. https://doi.org/10.2202/1544-6115.1128

Zhou, Y., Sun, W., Cai, H., Bao, H., Zhang, Y., Qian, G., & Ge, C. (2019). The role of anti-Müllerian hormone in testis differentiation reveals the significance of the TGF-β pathway in reptilian sex determination. *Genetics*, 213(4), 1317–1327. https://doi.org/10.1534/genetics.119.302527

SUPPORTING INFORMATION

Additional supporting information can be found online in the Supporting Information section at the end of this article.

How to cite this article: Gessler, T B., Wu, Z., & Valenzuela, N. (2023). Transcriptomic thermal plasticity underlying gonadal development in a turtle with ZZ/ZW sex chromosomes despite canalized genotypic sex determination. *Ecology and Evolution*, 13, e9854. https://doi.org/10.1002/ece3.9854